Article

Cell

A Sacrifice-for-Survival Mechanism Protects Root Stem Cell Niche from Chilling Stress

Graphical Abstract

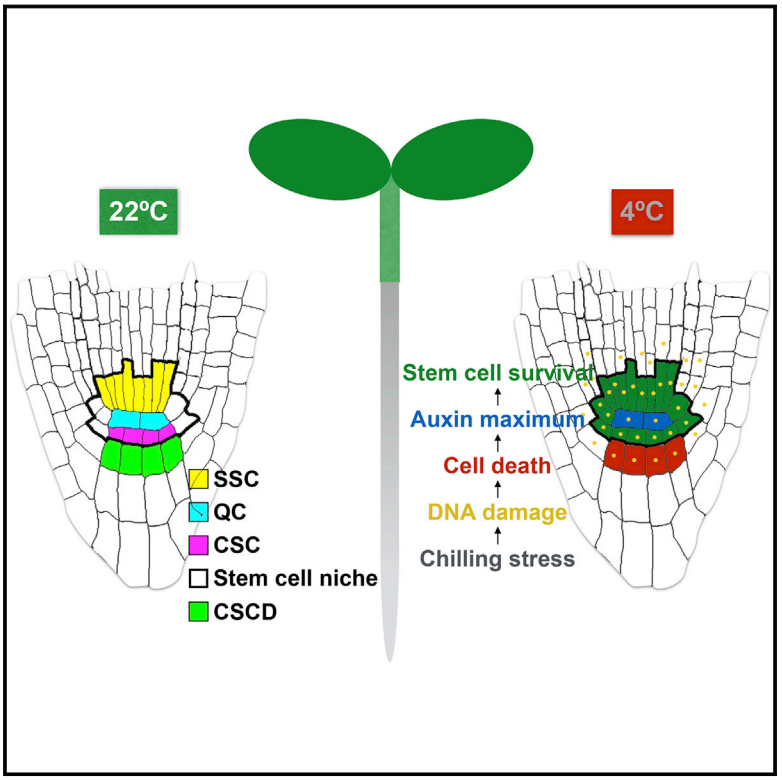

Highlights

- Chilling stress causes DNA damage in root stem cells and their early descendants
- Chilling stress induces protective death of columella stem cell daughters (CSCDs)
- CSCD death re-establishes QC auxin maximum and prevents further division of CSCs
- CSCD death improves the root's ability to withstand other stresses and to recover

Authors

Jing Han Hong, Maria Savina, Jing Du, ..., Wei Shi Sim, Victoria V. Mironova, Jian Xu

Correspondence

dbsxj@nus.edu.sg

In Brief

Arabidopsis roots protect their stem cell niche from chilling stress via a selective cell death mechanism regulated by auxin and DNA damage response.

Hong et al., 2017, Cell *170*, 1–12
June 29, 2017
http://dx.doi.org/10.1016/j.cell.2017.06.002

CellPress

Please cite this article in press as: Hong et al., A Sacrifice-for-Survival Mechanism Protects Root Stem Cell Niche from Chilling Stress, Cell (2017), http://dx.doi.org/10.1016/j.cell.2017.06.002

Article

Cell

A Sacrifice-for-Survival Mechanism Protects Root Stem Cell Niche from Chilling Stress

Jing Han Hong,[1] Maria Savina,[2,3] Jing Du,[1,4] Ajay Devendran,[1,4] Karthikbabu Kannivadi Ramakanth,[1] Xin Tian,[1] Wei Shi Sim,[1] Victoria V. Mironova,[2,3] and Jian Xu[1,5,*]

[1]Department of Biological Sciences and Centre for BioImaging Sciences, National University of Singapore, Singapore 117543, Singapore
[2]Institute of Cytology and Genetics, Novosibirsk 630090, Russia
[3]Novosibirsk State University, LCT&EB, Novosibirsk 630090, Russia
[4]These authors contributed equally
[5]Lead Contact
*Correspondence: dbsxj@nus.edu.sg
http://dx.doi.org/10.1016/j.cell.2017.06.002

SUMMARY

Temperature has a profound influence on plant and animal development, but its effects on stem cell behavior and activity remain poorly understood. Here, we characterize the responses of the *Arabidopsis* root to chilling (low but above-freezing) temperature. Chilling stress at 4°C leads to DNA damage predominantly in root stem cells and their early descendants. However, only newly generated/differentiating columella stem cell daughters (CSCDs) preferentially die in a programmed manner. Inhibition of the DNA damage response in these CSCDs prevents their death but makes the stem cell niche more vulnerable to chilling stress. Mathematical modeling and experimental validation indicate that CSCD death results in the re-establishment of the auxin maximum in the quiescent center (QC) and the maintenance of functional stem cell niche activity under chilling stress. This mechanism improves the root's ability to withstand the accompanying environmental stresses and to resume growth when optimal temperatures are restored.

INTRODUCTION

All organisms have evolved to cope with various stresses in their environment, ensuring the optimal combination of proliferation and survival. One of the most important and frequently changing environmental stresses that an organism must be able to cope with is temperature stress, which is induced by sub- or supra-optimal temperatures. The negative effects of temperature stress on human, animal, and plant life have been well studied, however, we have little knowledge on how temperature stress impacts the properties of stem cells and/or their niches and how they respond to and recover from its effects.

Stem cells and their lineage-committed progenies are vital for the development and growth of multicellular organisms. The quiescence, self-renewal, and differentiation of stem cells are regulated not just by local signals from within the niche, but also by systemic signals from outside the tissue (Hsu and Fuchs, 2012; Scheres, 2007). In the model dicot plant *Arabidopsis thaliana* (*Arabidopsis*), the root stem cell niche is made of a central organizing center known as the quiescent center (QC) and one layer of adjacent stem cells surrounding it (Scheres et al., 2002). The behavior and activity of the QC and surrounding stem cells are determined by an auxin maximum in the QC, which is generated and stabilized by PINFORMED (PIN)-mediated auxin transport (Blilou et al., 2005; Grieneisen et al., 2007; Sabatini et al., 1999). Both low (4°C) and high (29°C) temperatures have been shown to alter PIN-mediated auxin transport in the *Arabidopsis* root (Hanzawa et al., 2013; Shibasaki et al., 2009), but what remains obscure is the effects of temperature stress on the maintenance of the auxin maximum and the integrity of the stem cell niche.

Many plants, including *Arabidopsis* (Gilmour et al., 1988), develop a greater ability to withstand freezing after they have been exposed to a short period, usually 1 or 2 days, of chilling stress induced by low but above-freezing temperatures (Hincha and Zuther, 2014; Sung and Amasino, 2005; Thomashow, 1999). This relatively quick response, termed cold acclimation, is necessary before plants can survive the colder temperatures of winter and ensures that plants recover and flourish quickly in the spring. Up to now, however, little is known about the adaptive process of cold acclimation in the root stem cell niche, despite the fact that optimum root development and function are essential for bolstering plant growth and crop productivity under climate change (Den Herder et al., 2010; Gewin, 2010).

Here, we report, using the *Arabidopsis* root as a model system for study, that chilling stress (at 4°C) leads to DNA damage predominantly in the root stem cells and their early descendants and causes a loss of PIN-mediated auxin maximum in the QC after one round of the division of the columella stem cells (CSCs). To maintain the integrity of QC and root stem cells under chilling stress, an ataxia telangiectasia mutated (ATM), ATM and RAD3-related (ATR), and WEE1-mediated DNA damage response pathway is activated that induces death of newly generated/differentiating columella stem cell daughters (CSCDs) and so disrupts the directional flow of auxin, leading to the re-establishment of auxin maximum in the QC that preserves root stem cells in a quiescent state. This chilling stress-specific sacrifice-for-survival mechanism not only protects the stem cell niche from

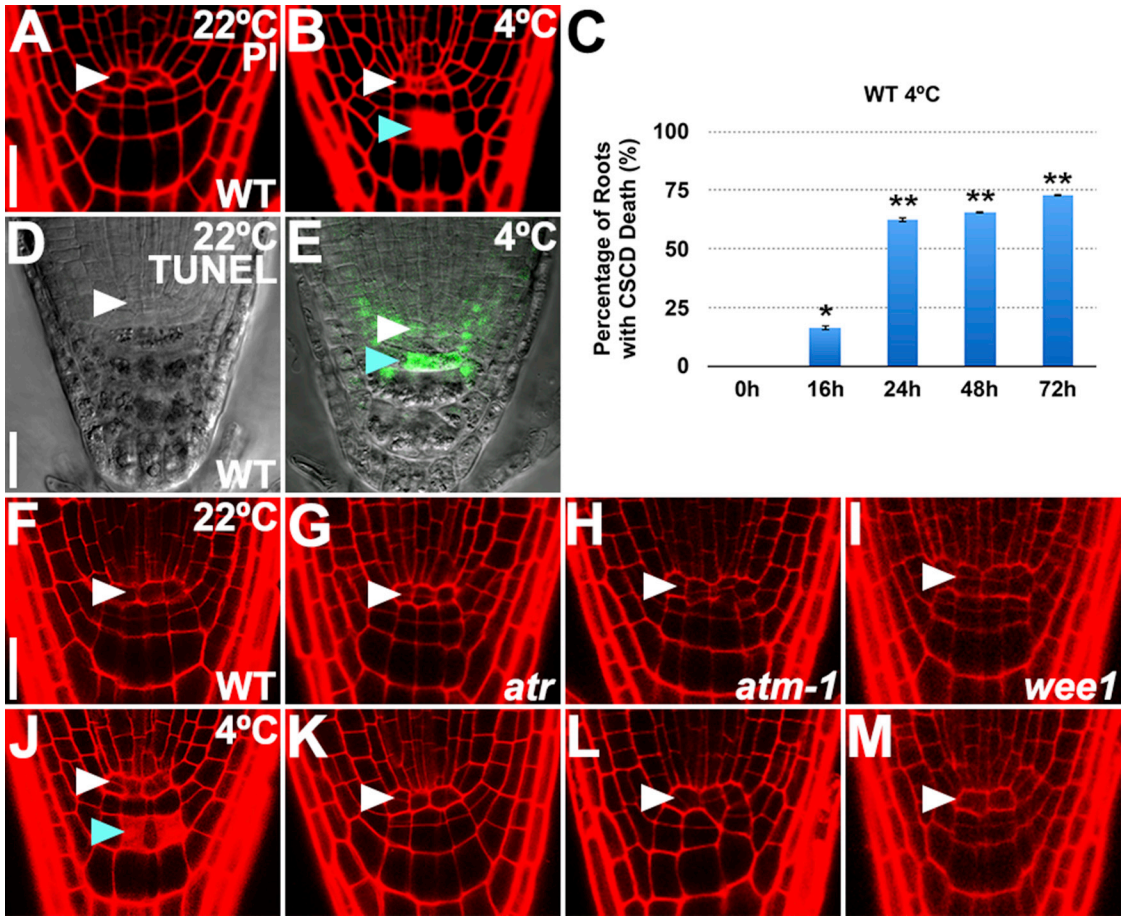

Figure 1. Chilling Stress Induces DNA Damage Response-Mediated Death of Columella Stem Cell Daughters

(A and B) Root tips of *Arabidopsis* wild-type (WT) seedlings exposed to the normal (22°C) (A) or chilling temperatures (4°C) (B) for 24 hr (24h). The death of columella stem cell daughters (CSCDs) was observed after 16h of exposure to chilling stress. Root cells were counterstained (in red) with propidium iodide (PI) and imaged with confocal microscopy. PI is excluded from entering live cells but penetrated into dead cells. White arrowhead points to the QC and blue arrowhead points to the dead CSCDs. Scale bar, 20 μm.

(C) Time course analysis of frequency of chilling stress-induced CSCD death over a period of 72 hr. The percentage of roots with CSCD death reached 60% to 70% after 24 hr and did not increase significantly thereafter. Error bars represent SEM. *$p < 0.05$ and **$p < 0.01$, t test, compared to 0 hr ($n = 3$ biological replicates).

(D and E) TUNEL assay of DNA fragmentation (stained in green) in root tip cells of WT seedlings exposed to the normal (22°C) (D) or chilling temperatures (4°C) (E) for 24 hr. White arrowhead points to the QC and blue arrowhead points to the CSCDs. Scale bar, 20 μm.

(F–M) Root tips of WT (F and J), *atr* (G and K), *atm-1* (H and L), *wee1* (I and M) seedlings exposed to the normal (22°C) (F–I) or chilling temperatures (4°C) (J–M) for 24 hr. The percentage of mutant roots with CSCD death were significantly lower than that of WT, suggesting that chilling stress-induced CSCD death is dependent on a functional DNA damage response. White arrowhead points to the QC and blue arrowhead points to the dead CSCDs. Scale bar, 20 μm.

See also Figure S1.

chilling stress but also improves the root's ability to withstand the accompanying environmental stresses and to recover when ambient temperatures rise to the optimal levels.

RESULTS

CSCDs Are Particularly Vulnerable to DNA Damage Induced by Chilling Stress

To assess the responses of root stem cells to chilling stress, *Arabidopsis* seedlings were exposed to control (22°C) or low but above-freezing temperature (4°C) for different durations before analysis. After 16 hr at 4°C, CSCDs of ~20% of seedling roots were found to take up propidium iodide (PI), which is able to enter dead cells but are impermeable to live cells (Figures 1A–1C). At 24 hr after chilling stress, the percentage of roots with dead CSCDs increased to ~60% to 70% and until 72 hr, the percentage did not increase significantly (Figure 1C). Over the course of a 72-hr study, chilling stress-induced death of the QC and stem cells was also observed but at a much lower frequency (Figure S1A), suggesting that CSCDs are particularly vulnerable when exposed to chilling stress.

Previous studies have shown that exposure of tobacco BY-2 cells (Koukalová et al., 1997) or maize root tip cells (Ning et al., 2002) to prolonged periods (1 week or more) of chilling stress

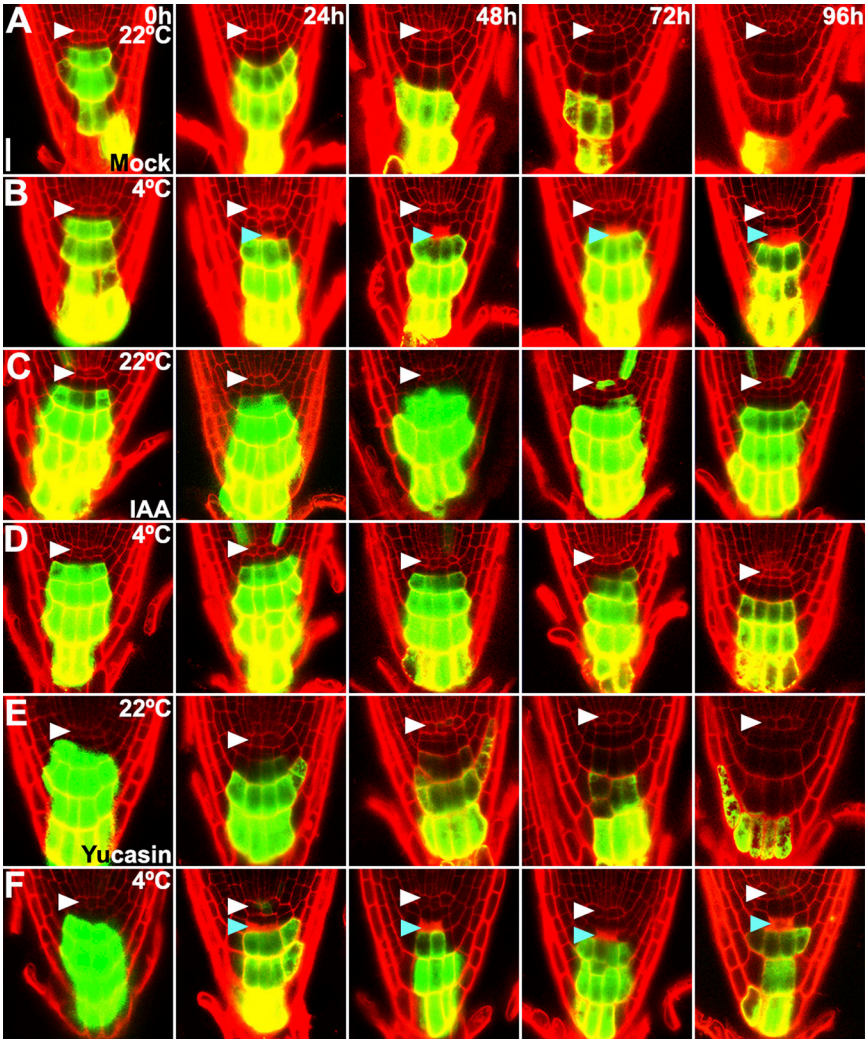

Figure 2. Auxin Levels Determine the Quiescence of CSCs and the Viability of Newly Generated/Differentiating CSCDs

(A–F) Root tips of *PIN3::CRE-GR 35S::LoxP-Ter-LoxP-VENUS* seedlings treated with mock (A and B), 1 nM IAA (C and D), or 50 nM yucasin (E and F). These seedlings were transferred to DEX-free medium after the induction of VENUS expression with 5 μM DEX at 22°C and allowed to grow at 22°C (A, C, E) or 4°C (B, D, F) for the indicated period of time. White arrowhead points to the QC and blue arrowhead points to the dead CSCDs. Scale bar, 20 μm. Note that upon chilling stress at 4°C, a single round of CSC division occurred within 24 hr, which was accompanied by the death of newly generated/differentiating CSCDs. As a result, additional rounds of CSC division were largely prevented. In the presence of 1 nM IAA, both CSC division and CSCD death were largely prevented.

See also Figures S2, S3, and S4.

led to DNA fragmentation and programmed cell death. Using terminal deoxynucleotidyl transferase (TdT)-mediated 2'-deoxyuridine 5'-triphosphate (dUTP) nick end labeling (TUNEL), we investigated the occurrence of DNA fragmentation in *Arabidopsis* root cells subjected to chilling stress for 24 hr. Intriguingly, TUNEL-positive nuclei were detected predominantly in root stem cells and their early descendants (Figures 1D and 1E), indicating that these cells are prone to DNA damage induced by chilling stress. Moreover, γ-H2AX foci, a highly sensitive marker for the detection of DNA damage induced by double strand breaks in DNA (Mah et al., 2010), were increasingly observed from 12 hr to 24 hr after chilling stress at 4°C (Figures S1C–S1H), but were less detected in loss-of-function mutants of ATR and ATM that phosphorylate H2AX to yield γ-H2AX in response to DNA damage (Maréchal and Zou, 2013) (Figures S1I and S1J). These findings suggest that chilling stress-induced death of CSCDs involves a functional DNA damage response mediated by ATR, ATM, and their downstream targets. Consistent with this hypothesis, in *atr*, *atm-1*, and *wee1* mutants, which are unable to efficiently transduce DNA damage signals (Culligan et al., 2004; De Schutter et al., 2007; Fulcher and Sablowski, 2009; Garcia et al., 2003), chilling stress-induced DNA damage (Figures S1K–S1M) could barely trigger the death of CSCDs (Figures 1F–1M and S1B).

A Single Round of CSC Division Occurs during Chilling Stress followed by Death of Newly Generated CSCDs

Unlike other stem cell daughters, CSCDs do not have the ability to divide and are committed for differentiation (Bennett et al., 2014; Dolan et al., 1993; Hong et al., 2015). We thus hypothesized that differentiating CSCDs are more sensitive to chilling stress-induced DNA damage than undifferentiated or fully differentiated cells. To test this hypothesis, we generated a synthetic tracking system (*PIN3::CRE-GR 35S::LoxP-Ter-LoxP-VENUS*) that, upon induction by dexamethasone (DEX), marks fully differentiated columella root cap cells with 35S promoter-driven constitutive expression of the fluorescent protein VENUS. As a result, newly generated or newly differentiated columella root cap cells are VENUS-free after removal of DEX, allowing the occurrence of CSC division and the phenotype of newly generated CSCDs to be readily determined.

An average increase in the number of VENUS-free columella root cap layer was observed every 24 hr through the 96 hr test at 22°C (Figures 2A and S2A), indicating the occurrence of multiple rounds of CSC division. By contrast, at 4°C only a single round of CSC division could possibly occur (Figures 2B and S2B) and, in agreement with our hypothesis, cell death was observed only when new CSCDs were generated (Figure 2B). Moreover, the death of newly-generated/differentiating CSCDs was not accompanied by a change in the cell-specific expression pattern of CSC (*J2341*; Figure S3A) and QC

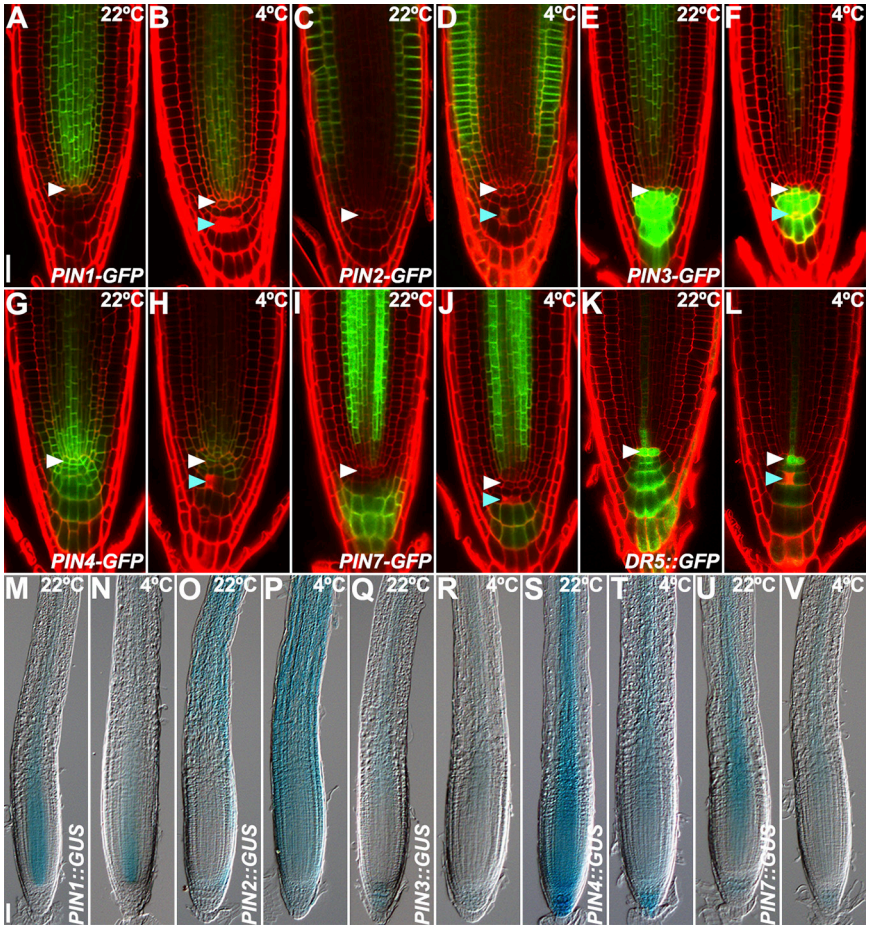

Figure 3. Chilling Stress Alters the Expression of *PIN::PIN-GFP*, *PIN::GUS*, and *DR5::GFP*

(A–L) Expression of *PIN1::PIN1-GFP* (A and B), *PIN2::PIN2-GFP* (C and D), *PIN3::PIN3-GFP* (E and F), *PIN4::PIN4-GFP* (G and H), *PIN7::PIN7-GFP* (I and J), and *DR5::GFP* (K and L) in the root tip of *Arabidopsis* seedlings exposed to the normal (22°C) (A, C, E, G, I, K) or chilling temperatures (4°C) (B, D, F, H, J, L) for 24 hr. White arrowhead points to the QC and blue arrowhead points to the dead CSCDs. Scale bar, 20 μm.

(M–V) Expression of *PIN1::GUS* (M and N), *PIN2::GUS* (O and P), *PIN3::GUS* (Q and R), *PIN4::GUS* (S and T), and *PIN7::GUS* (U and V) in the root tip of *Arabidopsis* seedlings exposed to the normal (22°C) (M, O, Q, S, U) or chilling (4°C) (N, P, R, T, V) temperatures for 24 hr. Scale bar, 50 μm.

See also Model Figures 2 and 3 of Data S1.

(*WOX5:: GFP*; Figure S3B) markers, indicating that QC cells and CSCs could maintain their identities under chilling stress.

Auxin Regulates Division of CSCs and Occurrence of CSCD Death under Chilling Stress

Division of cells in the root stem cell niche is regulated by an auxin maximum in the QC and by a local auxin gradient at the root tip, which is generated and stabilized by PIN-mediated auxin transport (Grieneisen et al., 2007). Chilling stress was previously reported to inhibit PIN2 and PIN3 expression as well as basipetal auxin transport in the *Arabidopsis* root (Shibasaki et al., 2009), indicating that the observed phenotypes of CSCs and CSCDs might be due to chilling stress-induced changes in auxin levels and distribution.

We found that the single round of CSC division occurred within the first 24 hr of chilling stress was largely blocked by addition of as low as 1 nM indole-3-acetic acid (IAA; a natural auxin) (Figures 2C, 2D, S2A–S2D, S4A, S4B, S4D, S4E, and S4G) and, as a result, a significantly low percentage of CSCD death was observed (Figures 2D and S4H) despite the presence of chilling stress-induced DNA damage (Figure S1N). Conversely, when IAA biosynthesis was inhibited by 50 nM yucasin (Nishimura et al., 2014), a higher incidence of CSC division and CSCD death was noted at 4°C (Figures 2E, 2F, S2A, S2B, S2E, S2F, S4A, S4C, S4D, S4F, S4G, and S4I). But ATR, ATM, and WEE1-mediated DNA damage response remained indispensable for the induction of CSCD death (Figures S1B and S1O–S1V). These findings confirm the first part of our hypothesis that chilling stress-induced changes in root tip auxin levels would contribute to the induction of CSC division and CSCD death. More importantly, our results suggest that auxin can be applied to promote the quiescence of CSCs and subsequently prevent the occurrence of CSC division and CSCD death under chilling stress.

CSCD Death Re-establishes the Auxin Maximum in the QC and, as a Result, Protects the Root Stem Cell Niche from Chilling Stress

We next asked whether chilling stress acts through modification of auxin distribution to trigger CSCD death. To this end, we explored the effect of chilling stress and the consequences of CSC division and CSCD death on root tip auxin distributions both in vivo and in silico, using an iterative experimental and computational approach.

After 24 hr at 4°C, expression levels of *PIN::PIN-GFP* and *PIN::GUS* displayed pronounced changes compared with the controls at 22°C (Figures 3A–3V, see also Model Figures 2 and 3 of Data S1). Chilling stress increased the expression of *PIN2::PIN2-GFP* (Figures 3C and 3D) and *PIN2::GUS* (Figures 3O and 3P) but reduced the expression of other *PIN::PIN-GFP* and *PIN::GUS* including *PIN1::PIN1-GFP* (Figures 3A and 3B), *PIN3::PIN3-GFP* (Figures 3E and 3F), *PIN4::PIN4-GFP* (Figures 3G and 3H), *PIN7:PIN7-GFP* (Figures 3I and 3J), *PIN1::GUS* (Figures 3M and 3N), *PIN3::GUS* (Figures 3Q and 3R), *PIN4::GUS* (Figures 3S and 3T), and *PIN7:GUS* (Figures 3U and 3V). These changes were associated with an overall reduction in the

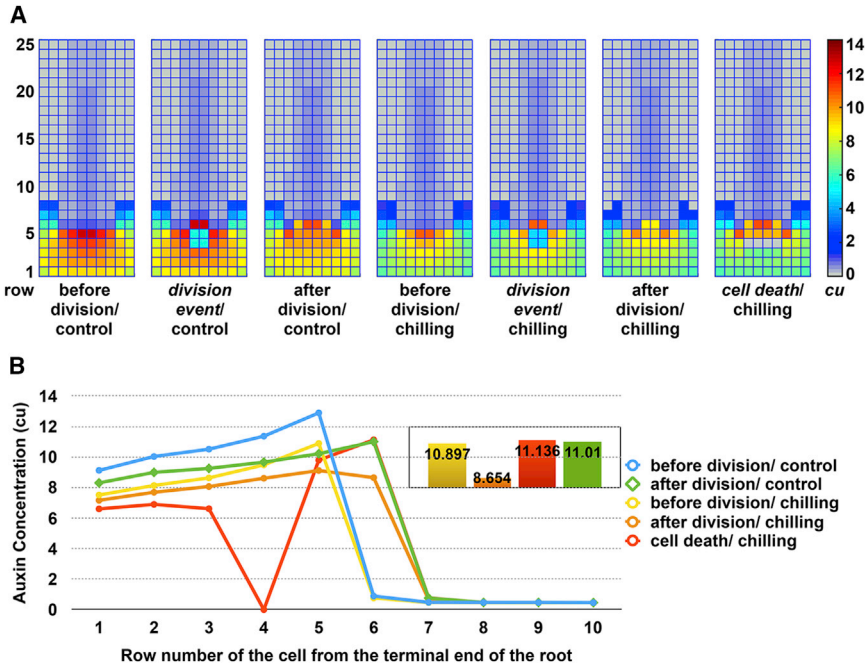

Figure 4. Simulation of Effects of CSC Division and CSCD Death on Auxin Distribution in the Root Tip

(A) From left to right: auxin distribution in control roots before CSC division, soon after it, and after an adaptation period; auxin distribution in chilling-stressed roots before CSC division, soon after it, after an adaptation period, and after CSCD death. The central two cells in row 5 represent the QC cells, and the central four cells in row 3 represents the CSCD cells. After CSC division, row 6 represents the QC, and row 4 represents the new CSCD cells.

(B) Cellular auxin concentrations in the central layer of the in silico root tip. Steady-state model solutions were evaluated for control roots before and after CSC division, for chilling-stressed roots before and after CSC division, and after CSCD death. The inset chart on the upper right shows the calculated QC auxin concentrations in chilling-stressed roots before and after CSC division, after CSCD death, and in control roots after CSC division.

See also Data S1.

expression of the auxin responsive *DR5::GFP* (Figures 3K and 3L) while the *DR5::GFP* expression maximum in the QC was maintained (Figures 3K and 3L). Thus, our results suggest that the primary root of *Arabidopsis*, when exposed to chilling stress, has the ability to maintain the auxin maximum in the QC, which is essential for the maintenance of the QC and stem cell integrity.

We next fed the observed *PIN::PIN-GFP* and *PIN::GUS* expression changes into a dual-mechanism model (Mironova et al., 2012) and simulated the consequences of CSC division and CSCD death on PIN-mediated auxin re-distribution in the root tip exposed to chilling stress (Figures 4A and 4B; Data S1). Consistent with the experimental findings obtained from the analysis of *DR5::GFP* expression (Figures 3K and 3L), in silico analysis showed that differential changes in *PIN::PIN-GFP* and *PIN::GUS* expression led to a new steady-state equilibrium of auxin distribution in chilling-stressed root, despite an overall decline in auxin levels (Figures 4A and 4B). In this new steady state, however, the division of CSCs caused a loss of auxin maximum in the QC (Figures 4A and 4B), which could be restored only if the death of newly generated/differentiating CSCDs occurred (Figures 4A and 4B). By contrast, CSC division at normal temperature had no effect on the maintenance of auxin maximum in the QC (Figures 4A and 4B). These results together indicate that under chilling stress, the death of newly generated/differentiating CSCDs is necessary for the re-establishment of auxin maximum in the QC.

In agreement with our model prediction that CSCD death increases the auxin concentration in the QC (Figure 4B, inset chart), roots with chilling stress-induced CSCD death displayed a higher *DR5::GFP* (Figures 5A, 5B, and S3C) and *WOX5::GFP* expression (Figures 5C, 5D, and S3D) in the QC than those without. We thus concluded that CSCD death was the strategy used by the root to sustain the auxin maximum (as indicated by *DR5::GFP*) in the QC and so maintain the associated QC activity (as indicated by *WOX5::GFP*) under chilling stress. To further evaluate the role of CSCD death in the maintenance of integrity of QC and root stem cells under chilling stress, we used the DEX-inducible *GAL4-VP16-GR* (*GVG*)/*UAS* system and the artificial microRNA (amiRNA) technology (Schwab et al., 2006) to achieve an inducible downregulation in *ATR*, *ATM*, and *WEE1* expression specifically in *ARABIDOPSIS CRINKLY 4* (*ACR4*)-expressing cells (including QC cells, CSCs and CSCDs) (De Smet et al., 2008), which we expected to suppress DNA damage signal transduction and consequently inhibit CSCD death. As expected, we found that chilling stress-induced death of CSCDs was markedly reduced in *ACR4::GVG-UAS::ATRi* (*ATRi*), *ACR4::GVG-UAS::ATMi* (*ATMi*), and *ACR4::GVG-UAS::WEE1i* (*WEE1i*) seedlings grown on the DEX-containing medium (Figures 5E–5L and S5F). The reduction of CSCD death in these seedlings was accompanied by an increase of cell division (Figures S5A–S5E) and cell death in the root stem cell niche (Figures 5I–5L and S5F), strongly suggesting that death of CSCDs under chilling stress prevents division and consequent death of root stem cells.

Interestingly, we found that chilling stress-induced death of CSCDs rendered QC and root stem cells less sensitive to zeocin (30 μg/mL at 4°C) (Figures 5M, 5N, S6A, S6F, S6I, and S6L), a genotoxin previously reported to cause preferential death of stele stem cells (SSCs) and CSCs (to a lesser extent) (Fulcher and Sablowski, 2009; Zhang et al., 2016). Moreover, 50 nM IAA could largely prevent the death of these cells in roots exposed to zeocin (5 μg/mL at 22°C) (Figures 5O, 5P, and S6B), whereas genetic (using *yuc8 yuc9* double mutants) (Hentrich et al., 2013) and pharmacological (using 200 nM yucasin) disruption of auxin biosynthesis sensitized these cells to zeocin (5 μg/mL at 22°C and 30 μg/mL at 4°C) (Figures S6C–S6L), in particular when

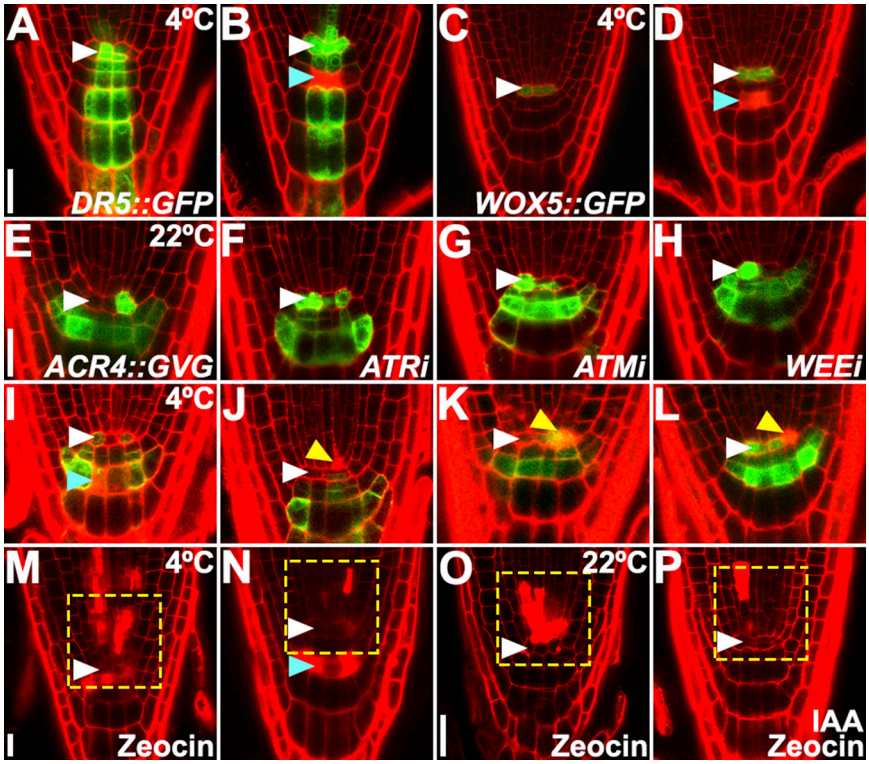

Figure 5. Death of CSCDs Maintains Auxin Maximum in the QC and Protects QC and Stem Cell Integrity

(A–D) Expression of *DR5::GFP* (A and B) and *WOX5::GFP* (C and D) in the QC of *Arabidopsis* roots without (A and C) or with (B and D) chilling stress-induced CSCD death. White arrowhead points to the QC and blue arrowhead points to the dead CSCDs. Scale bar, 20 μm.

(E–L) Root tips of DEX (5 μM)-treated *ACR4::GVG* (E and I), *ATRi* (F and J), *ATMi* (G and K), and *WEE1i* (H and L) seedlings exposed to normal (22°C) (E–H) or chilling temperatures (4°C) (I–L) for 24 hr. Note that DEX-induced knockdown of *ATR*, *ATM*, and *WEE1* in *ACR4*-expressing cells (including CSCs and CSCDs) largely prevents death of CSCDs but sensitizes root stem cells to chilling stress. White arrowhead points to the QC and blue arrowhead points to the dead CSCDs. Scale bar, 20 μm.

(M and N) Root tips of WT seedlings without (M) or with (N) chilling stress-induced CSCD death. Following 24 hr of chilling stress at 4°C, these seedlings were treated with 30 μg/mL zeocin at 4°C for 24 hr before imaging. White arrowhead points to the QC. Blue and yellow arrowheads point to the dead CSCDs and dead stem cells, respectively. Box regions show the death of QC cells, root stem cells, and their early descendants. Scale bar, 20 μm.

(O and P) Root tips of WT seedlings treated with 5 μg/mL zeocin (O) or 5 μg/mL zeocin and 50 nM IAA (P) for 24 hr at 22°C. Box regions show the death of QC, root stem cells, and their early descendants. White arrowhead points to the QC. Box regions show the death of QC cells, root stem cells, and their early descendants. Scale bar, 20 μm.

See also Figures S3, S5, and S6.

chilling stress-induced CSCD death was absent (Figures S6F–S6H and S6L compared to Figures S6I–S6L). Together, these findings demonstrate the importance of auxin level in the protection of root stem cell integrity and indicate that chilling stress-induced death of CSCDs results in an increase of auxin levels in the root stem cell niche, which prevents division and consequently death of root stem cells caused by additional environmental stresses that damage DNA.

Death of CSCDs Helps Prepare the Root to Withstand the Accompanying Environmental Stresses and to Recover Faster When Returned to Optimal Temperatures

Using the *PIN3::CRE-GR 35S::LoxP-Ter-LoxP-VENUS* system, we next examined whether the death of CSCDs impacts on the recovery of CSC division at the optimal growth temperature. When chilling-stressed *Arabidopsis* seedlings were exposed to 22°C, we observed a significantly higher rate of CSC division in roots with CSCD death compared to those without (Figures 6A–6H and S3E). This finding indicates that death of CSCDs enables roots to maintain a functional stem cell pool under chilling stress and to recover faster after chilling stress. Consistently, we found that CSCD death or auxin (1 nM IAA) significantly increased the root growth recovery rate from chilling stress when compared to roots without CSCD death (Figures S4J and S5G). By contrast, yucasin (50 nM) and DEX-induced knockdown of *ATM*, *ATR*, and *WEE1* in *ACR4*-expressing cells, both of which sensitized root stem cells to cell death (Figures 5I–5L, S5F, and S6), resulted in a significantly compromised recovery of root growth from chilling stress (Figures S4J and S5G).

We next asked whether the death of CSCDs also helps prepare roots to withstand freezing temperature, hence allowing for greater recovery of root growth when returned to normal temperature. To answer this question, chilling-stressed seedlings were incubated at 0°C for 7 days and then transferred to 22°C for another 7 days before root growth was evaluated. Our data showed that roots with CSCD death could increase their length more rapidly than those without (Figures 6I, 6L, and S5H), suggesting that there could be a direct link between CSCD death and root growth rescue in a subsequent freezing treatment. To test this possibility, we mimicked the chilling stress-induced death of CSCDs with the ablation of CSCDs using a multi-photon laser. We found that CSCD ablation (Figures S7A–S7D) led to a significant increase of *DR5::GFP* expression in the QC (Figures S7C–S7E) and a better recovery of root growth from freezing stress without a prior chilling treatment (Figures S7F and S7G), thus establishing CSCD death as an integral part of an auxin-mediated root growth adaptive process of cold acclimation. Moreover, by inducing auxin biosynthesis specifically in the QC, through providing the *WOX5::IAAH DR5::GFP* seedlings with the auxin precursor indole-3-acetamide (IAM) that can be converted by the IAM hydrolase (IAAH) to IAA (Blilou et al.,

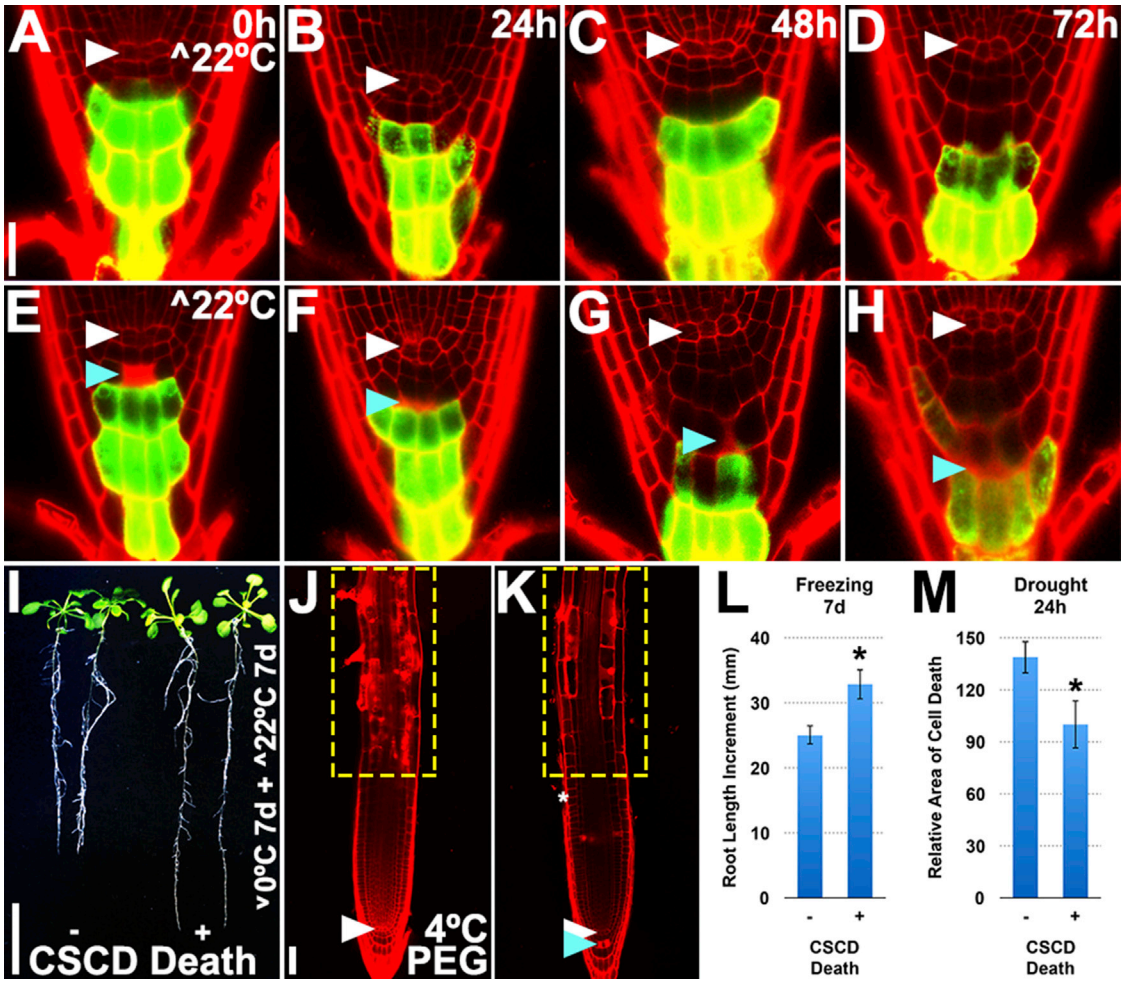

Figure 6. Death of CSCDs Enables the Root to Withstand the Accompanying Environmental Stresses and to Recover Faster When Returned to Optimal Temperatures

(A–H) Root tips of *PIN3::CRE-GR 35S::LoxP-Ter-LoxP-VENUS* seedlings, which were transferred to DEX-free medium after the induction of *VENUS* expression with 5 μM DEX at 22°C and chilling-stressed at 4°C for 24 hr. The seedlings without (A–D) and with (E–H) chilling stress-induced CSCD death were then allowed to recover at 22°C for the indicated period of time before imaging. White arrowhead points to the QC and blue arrowhead points to the dead CSCDs. Scale bar, 20 μm.

(I and L) WT seedlings without (–) or with (+) chilling stress-induced CSCD death. Following 24 hr of chilling stress at 4°C, these seedlings were freezing-stressed at 0°C for 7 days and then allowed to recover at 22°C for another 7 days before imaging (I) and quantification (L). Scale bar, 20 mm. Error bars in (L) represent SEM. *$p < 0.05$, t test ($n = 3$ biological replicates).

(J, K, and M) Root tips of WT seedlings without (–) (J) or with (+) (K) chilling stress-induced CSCD death. Following 24 hr of chilling stress at 4°C, these seedlings were drought (20% PEG6000)-stressed at 4°C for 24 hr before imaging (J and K) and quantification (M). White arrowhead points to the QC and blue arrowhead points to the dead CSCDs. Scale bar, 20 μm. Note that drought stress induces cell death specifically in the root elongation zone (boxed region). Error bars in (M) represent SEM. *$p < 0.05$, t test ($n = 3$ biological replicates).

See also Figures S4, S5, and S7.

2005), we further demonstrated a direct and positive correlation between auxin level and root growth recovery rate after freezing stress (Figures S7H–S7L).

It has been well known that when plants are cold-acclimated, they also show an elevated tolerance to drought (Siminovitch and Cloutier, 1983; Steponkus, 1979). We, therefore, examined whether there is a correlation between CSCD death and drought tolerance. Twenty-four hours of exposure of chilling-stressed seedlings to polyethylene glycol (20% of PEG-6000 at 4°C), which has been effectively used to mimic drought stress (Hohl and Schopfer, 1991), caused death of root cells predominantly in the elongation zone (Figures 6J and 6K), indicating that these cells are particularly vulnerable to drought stress. Quantification of the area of cell death in the elongation zone showed that roots with CSCD death had significantly lower levels of elongation zone cell death than those without (Figure 6M). This finding suggests that CSCD death could reduce the extent of the damage caused by drought. Thus, the death of CSCDs under chilling stress renders the root the ability to withstand the accompanying environmental stresses.

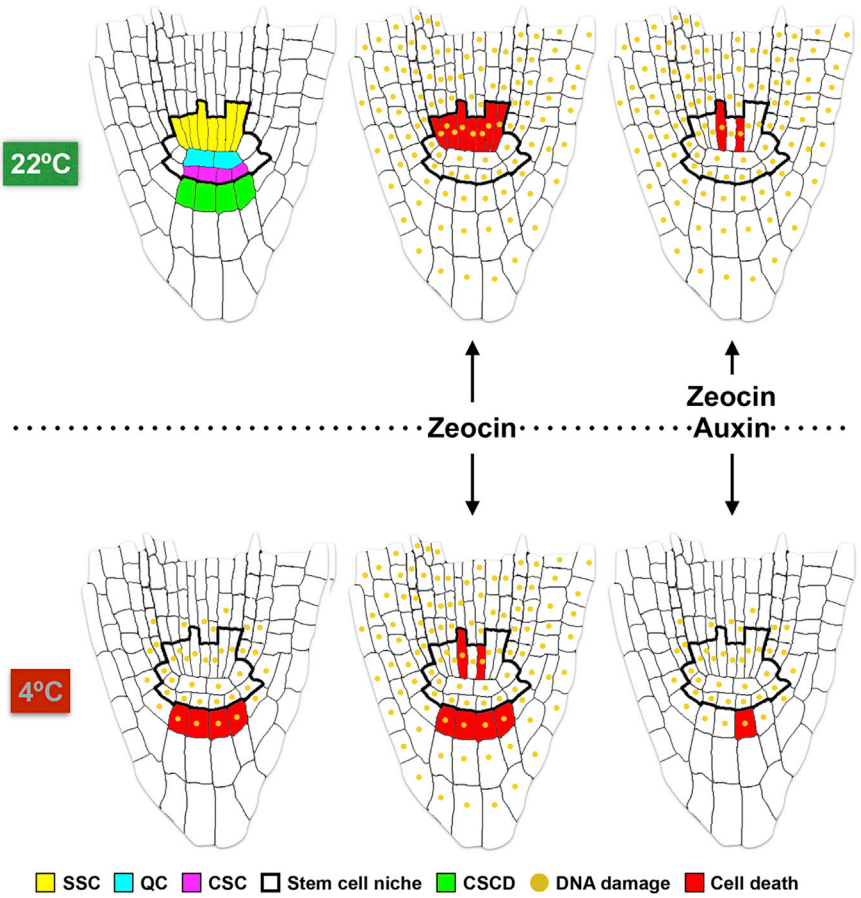

Figure 7. A Model for Life and Death Decisions of Root Stem Cells after DNA Damage under Normal and Chilling Temperatures

Cartoons show the medial longitudinal view of the *Arabidopsis* root tip, in which the root stem cell niche is outlined with a thick black border. Color codes in the root tips indicate cell fates. Yellow, SSC; blue, QC; magenta, CSC; green, CSCD; gold, DNA-damaged cell; red, dead cell. When root stem cells experience DNA damage, they are faced with the decision to live or to die in the larger interest of the health of the root vascular tissue. If DNA damage (for instance triggered by zeocin) occurs at physiological temperatures (e.g., 22°C, upper row), SSCs with unrepaired DNA will be eliminated to maintain genome integrity and normal functionality of root vascular tissue. Under suboptimal temperatures (e.g., 4°C, lower row), however, the preservation of stem cell pools is of central importance for plant survival and recovery. To protect SSCs and other root stem cells from chilling stress and the accompanying DNA-damaging stresses (for instance triggered by zeocin), the decision to sacrifice newly generated/differentiating CSCDs is made and executed, resulting in an anatomical block to auxin transport and so preventing the loss of the auxin maximum in the QC after CSC division under chilling stress. Auxin, which is essential for QC activity and stem cell quiescence, thus contributes significantly to root stem cell survival in response to DNA-damage in both normal and chilling temperatures.

DISCUSSION

A Chilling Stress-Specific Sacrifice-for-Survival Mechanism for Maintenance of the Root Stem Cell Niche

In the present study, we used an iterative experimental and computational approach to identify critical developmental and physiological processes that help shape a chilling stress-specific sacrifice-for-survival mechanism in the *Arabidopsis* root. The dicot model *Arabidopsis* is conventionally classified as a chilling-resistant plant (Kratsch and Wise, 2000) due to its lack of chilling stress-induced cell injury in leaf tissues (Hugly and Somerville, 1992). However, our analysis of root phenotypes of chilling-stressed wild-type (Col-0) *Arabidopsis* plants by confocal laser scanning microscope revealed that chilling stress could induce cell injury in the root tip. More specifically, we found that *Arabidopsis* root stem cells and their early descendants were highly prone to chilling stress-induced DNA damage and, among them, only CSCDs displayed a high rate of death that is mediated by the canonical DNA damage response proteins ATR, ATM, and WEE1. This finding indicates that chilling stress-induced DNA damage is necessary but not sufficient to trigger cell death and that induction of cell death after DNA damage is cell-type-dependent.

Only a single round of CSC division occurred during the 96-hr period of chilling stress and only newly generated/differentiating CSCDs underwent cell death. These findings imply that induction of cell death after chilling stress-induced DNA damage is dependent on both cell division and cell differentiation. Based on earlier findings (Shibasaki et al., 2009), we hypothesized and confirmed that chilling stress leads to dynamic changes in PIN-regulated auxin level and distribution in the *Arabidopsis* root, which is decisive for CSC division and occurrence of CSCD death. Moreover, with the help of computational simulations generated using a dual-mechanism model modified from our earlier work (Mironova et al., 2012), we demonstrated that death of newly generated/differentiating CSCDs provides an anatomical block to auxin transport and so re-establish the auxin maximum in the QC. This prevents the loss of QC activity and root stem cell quiescence and as such protects the root stem cell niche from chilling stress.

More importantly, we discovered that death of CSCDs is used as a broad-spectrum adaptation and survival strategy in chilling-stressed roots (Figure 7), which renders roots the ability to withstand and recover faster and better from chilling and freezing stress and offers protection against the damaging effects of the radiomimetic chemical zeocin on root stem cells and PEG-induced drought stress on root elongation zone cells. This finding provides an opportunity to explore how cold acclimation improves tolerance of many plant species to freezing and drought stresses (Seki et al., 2002; Siminovitch and Cloutier, 1983; Steponkus,

1979), which may help breeding efforts aimed at reducing the impact of these environmental stresses on crop productivity.

Significance of Auxin- and DNA Damage Response-Dependent Selective Cell Death in Plant Responses to DNA-Damaging Environmental Stresses

Understanding the biological significance of selective cell death in response to different DNA damage-inducing stresses has been a challenge for biologists for decades. In plants, roots stem cells and their early descendants were previously reported to be selectively killed by mild treatment with UV light, ionizing radiation, and radiomimetic drugs (Curtis and Hays, 2007; Fulcher and Sablowski, 2009; Furukawa et al., 2010; Heyman et al., 2013; Zhang et al., 2016). However, in all these reports, SSCs but not CSCDs appear to be the most vulnerable to DNA damage. Moreover, while ATR- and ATM-mediated DNA damage response is required to trigger the death of both SSCs and CSCDs, WEE1 does not seem to contribute to the death of SSCs (Fulcher and Sablowski, 2009). These findings suggest that the signal transduction pathways between DNA damage and cell death are different in SSCs and CSCDs.

Why would plants use different strategies to either kill or protect SSCs and other stem cells in the root stem cell niche? The lower sensitivity of chilling-stressed roots to zeocin suggests that the choice of life and death is made dependent on their external environment (Figure 7). During physiological conditions when rapid cell division occurs, a plausible advantage of eliminating DNA-damaged SSCs may be to prevent mutations resulting from unrepaired DNA damage, thus maintaining a functional root vascular tissue that is vital for the ability of the root to transport water, minerals, and hormones within the plant and for the growth and survival of the plant (Heo et al., 2017). A similar argument may apply to the protection of SSCs and other stem cells in roots under chilling temperatures or other adverse environmental conditions, after which a fast recovery of root tissues is dependent on the presence of a functional stem cell pool.

An interesting finding that emerged from this study was that death of both root stem cells and CSCDs could be largely inhibited by low levels of IAA, which indicates that the phytohormone auxin acts as a key regulator of DNA damage-triggered selective cell death in plants (Figure 7). While a link between auxin and DNA damage-triggered selective cell death has not been established previously, our literature review revealed the possible existence of such a link in plant responses to bacterial pathogens that induce hypersensitive cell death in leaves. First, diverse bacterial pathogens induce DNA damage in the genome of their host plants, which arises before the occurrence of hypersensitive cell death (Song and Bent, 2014). Second, auxin is able to suppress hypersensitive cell death (Chang et al., 2015) and negatively regulate plant immunity (Ludwig-Müller, 2015; Ma and Ma, 2016; Naseem et al., 2015). Third, hypersensitive cell death occurs in the bundle sheath cells surrounding the veins of a leaf (Morel and Dangl, 1997), where two auxin transporters, PIN3 and ABCB19/PGP19, function coordinately to control auxin transport to the vascular tissue (Bandyopadhyay et al., 2007; Blakeslee et al., 2007; Friml et al., 2002). Therefore, this death may influence local and global auxin transport and so regulate the defense responses of the plant in both local and distant tissues. Taken together, these data indicate that in addition to its well-documented role in controlling plant development and growth, auxin contributes significantly to cell survival in response to DNA damage triggered by both abiotic and biotic stresses.

A Stem Cell Model for the Understanding of Cold Adaption and Survival Strategies in Multicellular Organisms

More than 80% of the Earth's biosphere is permanently or seasonally subjected to temperatures below 5°C, which has a significant impact on the performance and geographical distribution of species. To maintain reproductive success and fitness, animals and plants must cope with low temperatures on a daily or seasonal basis. This challenge is made greater by climate change. Climate simulation, observation, and reanalysis data indicate that one of the consequences of worsening global warming is the frequent occurrence of colder and longer winters in northern mid-latitudes (Mori et al., 2014; Overland et al., 2016; Shepherd, 2016).

Chilling injury has been recognized as a unique environmental impact on crop plant physiology for over 90 years (Faris, 1926; Lyons, 1973). However, while the ultrastructural symptomology of chilling injury to photosynthetic tissues is well established in the literature (Kratsch and Wise, 2000), at the physiological level it remains unclear whether death of cells under chilling stress is merely an indication of cytotoxicity or occurs as one of the cold adaptation and survival strategies in plants. This is largely due to the lack of working models that allow for the dissection of developmental and physiological effects of chilling stress-induced injury. Our finding in the *Arabidopsis* root thus provides us a unique opportunity to identify and to study, at spatial and temporal resolutions, developmental and physiological responses that help shape cold adaptation and survival strategies in plants. Most importantly, we have now an excellent stem cell model to investigate specialized responses of the stem cell niche to chilling stress. The wide distribution of *Arabidopsis* accessions in northern hemisphere makes our model particularly suited for genetic dissection of complex molecular variation that has underpinned the successful adaptation of plant stem cells to cold environments.

Chilling injury has also been noted by many investigations in animals, such as in muscle tissue of the migratory locusts (MacMillan et al., 2015), in rat thymus (Morishita et al., 1997), and in mouse brain (Murakami et al., 1999). However, very little is known, particularly in mammalians, about the effects of chilling stress on stem cells and/or their niches and how they respond to its effects. Given that animal and plant stem cells are similar enough in terms of niche organization, behavior, and sensitivity to genotoxic stress (Fulcher and Sablowski, 2009; Heidstra and Sabatini, 2014; Heyman et al., 2013; Sablowski, 2004; Wang et al., 2012; Zhang et al., 2016), our CSCD death model may hold a promise to provide fundamental insights into understanding cold adaption and survival strategies across kingdoms.

STAR★METHODS

Detailed methods are provided in the online version of this paper and include the following:

- KEY RESOURCES TABLE

SUPPLEMENTAL INFORMATION

Supplemental Information includes seven figures, one table, and one data file and can be found with this article online at http://dx.doi.org/10.1016/j.cell.2017.06.002.

AUTHOR CONTRIBUTIONS

J.H.H. and J.X. designed the experiments. J.H.H., J.D., A.D., K.K.R., X.T. and W.S.S. carried out the experiments. V.V.M. designed and M.S. performed the computational simulations. J.X. and V.V.M. wrote the manuscript with input from J.H.H. and M.S. All the other authors discussed and commented on the final manuscript.

ACKNOWLEDGMENTS

We thank Ben Scheres for critical reading of the manuscript, Hao Yu and Toshiro Ito for helpful discussion, Fedor Kazantsev for technical support with the mathematical model, Yan Tong for technical support with the confocal microscope. Wai Shiu Fred Wong for γ-H2AX antibody, Li Zeng for TUNEL assay kit, Lieven De Veylder for *atm-1*, Kiyotaka Okada, Toshiaki Tameshige, and Michael Lenhard for providing *CG35ST_SKattB1-2* and *35S::LoxP-Ter-LoxP-VENUS*, Jim Haseloff for making available the CSC marker *J2341*, Yunde Zhao for the *yuc8 yuc9* double mutant, and the Nottingham Arabidopsis Stock Centre for providing *atr* (SALK_054383) and *wee1* (SALK_147968C). This work was supported by the AcRF Tier 2 grant (MOE2014-T2-1-128) from the Ministry of Education of Singapore, by the National Research Foundation Singapore under its Competitive Research Programme (CRP Award NRF2010NRF-CRP002-018 to J.X.), by the President's Graduate Fellowship of National University of Singapore (to J.H.H.), by the Russian Federation President Grant for Young Scientists (MK-1297.2017.4) and budget project 0324-2016-0008 (to V.M. and M.S.).

Received: November 23, 2016
Revised: April 24, 2017
Accepted: June 1, 2017
Published: June 22, 2017

REFERENCES

Bandyopadhyay, A., Blakeslee, J.J., Lee, O.R., Mravec, J., Sauer, M., Titapiwatanakun, B., Makam, S.N., Bouchard, R., Geisler, M., Martinoia, E., et al. (2007). Interactions of PIN and PGP auxin transport mechanisms. Biochem. Soc. Trans. *35*, 137–141.

Bennett, T., van den Toorn, A., Willemsen, V., and Scheres, B. (2014). Precise control of plant stem cell activity through parallel regulatory inputs. Development *141*, 4055–4064.

Blakeslee, J.J., Bandyopadhyay, A., Lee, O.R., Mravec, J., Titapiwatanakun, B., Sauer, M., Makam, S.N., Cheng, Y., Bouchard, R., Adamec, J., et al. (2007). Interactions among PIN-FORMED and P-glycoprotein auxin transporters in Arabidopsis. Plant Cell *19*, 131–147.

Blilou, I., Xu, J., Wildwater, M., Willemsen, V., Paponov, I., Friml, J., Heidstra, R., Aida, M., Palme, K., and Scheres, B. (2005). The PIN auxin efflux facilitator network controls growth and patterning in Arabidopsis roots. Nature *433*, 39–44.

Chang, X., Riemann, M., Liu, Q., and Nick, P. (2015). Actin as deathly switch? How auxin can suppress cell-death related defence. PLoS ONE *10*, e0125498.

Clough, S.J., and Bent, A.F. (1998). Floral dip: a simplified method for Agrobacterium-mediated transformation of Arabidopsis thaliana. Plant J. *16*, 735–743.

Culligan, K., Tissier, A., and Britt, A. (2004). ATR regulates a G2-phase cell-cycle checkpoint in Arabidopsis thaliana. Plant Cell *16*, 1091–1104.

Curtis, M.J., and Hays, J.B. (2007). Tolerance of dividing cells to replication stress in UVB-irradiated Arabidopsis roots: requirements for DNA translesion polymerases eta and zeta. DNA Repair (Amst.) *6*, 1341–1358.

De Schutter, K., Joubès, J., Cools, T., Verkest, A., Corellou, F., Babiychuk, E., Van Der Schueren, E., Beeckman, T., Kushnir, S., Inzé, D., and De Veylder, L. (2007). Arabidopsis WEE1 kinase controls cell cycle arrest in response to activation of the DNA integrity checkpoint. Plant Cell *19*, 211–225.

De Smet, I., Vassileva, V., De Rybel, B., Levesque, M.P., Grunewald, W., Van Damme, D., Van Noorden, G., Naudts, M., Van Isterdael, G., De Clercq, R., et al. (2008). Receptor-like kinase ACR4 restricts formative cell divisions in the Arabidopsis root. Science *322*, 594–597.

Dello Ioio, R., Nakamura, K., Moubayidin, L., Perilli, S., Taniguchi, M., Morita, M.T., Aoyama, T., Costantino, P., and Sabatini, S. (2008). A genetic framework for the control of cell division and differentiation in the root meristem. Science *322*, 1380–1384.

Den Herder, G., Van Isterdael, G., Beeckman, T., and De Smet, I. (2010). The roots of a new green revolution. Trends Plant Sci. *15*, 600–607.

Dolan, L., Janmaat, K., Willemsen, V., Linstead, P., Poethig, S., Roberts, K., and Scheres, B. (1993). Cellular organisation of the Arabidopsis thaliana root. Development *119*, 71–84.

Eriksson, S., Stransfeld, L., Adamski, N.M., Breuninger, H., and Lenhard, M. (2010). KLUH/CYP78A5-dependent growth signaling coordinates floral organ growth in Arabidopsis. Curr. Biol. *20*, 527–532.

Faris, J.A. (1926). Cold chlorosis of sugarcane. Phytopathology *16*, 885–891.

Friml, J., Wiśniewska, J., Benková, E., Mendgen, K., and Palme, K. (2002). Lateral relocation of auxin efflux regulator PIN3 mediates tropism in Arabidopsis. Nature *415*, 806–809.

Friml, J., Vieten, A., Sauer, M., Weijers, D., Schwarz, H., Hamann, T., Offringa, R., and Jürgens, G. (2003). Efflux-dependent auxin gradients establish the apical-basal axis of Arabidopsis. Nature *426*, 147–153.

Fulcher, N., and Sablowski, R. (2009). Hypersensitivity to DNA damage in plant stem cell niches. Proc. Natl. Acad. Sci. USA *106*, 20984–20988.

Furukawa, T., Curtis, M.J., Tominey, C.M., Duong, Y.H., Wilcox, B.W., Aggoune, D., Hays, J.B., and Britt, A.B. (2010). A shared DNA-damage-response pathway for induction of stem-cell death by UVB and by gamma irradiation. DNA Repair (Amst.) *9*, 940–948.

Garcia, V., Bruchet, H., Camescasse, D., Granier, F., Bouchez, D., and Tissier, A. (2003). AtATM is essential for meiosis and the somatic response to DNA damage in plants. Plant Cell *15*, 119–132.

Gewin, V. (2010). Food: An underground revolution. Nature *466*, 552–553.

Gilmour, S.J., Hajela, R.K., and Thomashow, M.F. (1988). Cold Acclimation in Arabidopsis thaliana. Plant Physiol. *87*, 745–750.

Grieneisen, V.A., Xu, J., Marée, A.F., Hogeweg, P., and Scheres, B. (2007). Auxin transport is sufficient to generate a maximum and gradient guiding root growth. Nature *449*, 1008–1013.

Hanzawa, T., Shibasaki, K., Numata, T., Kawamura, Y., Gaude, T., and Rahman, A. (2013). Cellular auxin homeostasis under high temperature is regulated through a sorting NEXIN1-dependent endosomal trafficking pathway. Plant Cell *25*, 3424–3433.

Heidstra, R., and Sabatini, S. (2014). Plant and animal stem cells: similar yet different. Nat. Rev. Mol. Cell Biol. *15*, 301–312.

Hentrich, M., Böttcher, C., Düchting, P., Cheng, Y., Zhao, Y., Berkowitz, O., Masle, J., Medina, J., and Pollmann, S. (2013). The jasmonic acid signaling pathway is linked to auxin homeostasis through the modulation of YUCCA8 and YUCCA9 gene expression. Plant J. *74*, 626–637.

Heo, J.O., Blob, B., and Helariutta, Y. (2017). Differentiation of conductive cells: a matter of life and death. Curr. Opin. Plant Biol. *35*, 23–29.

Heyman, J., Cools, T., Vandenbussche, F., Heyndrickx, K.S., Van Leene, J., Vercauteren, I., Vanderauwera, S., Vandepoele, K., De Jaeger, G., Van Der Straeten, D., and De Veylder, L. (2013). ERF115 controls root quiescent center cell division and stem cell replenishment. Science *342*, 860–863.

Hincha, D.K., and Zuther, E. (2014). Plant cold acclimation and freezing tolerance. Methods Mol. Biol. *1166*, 1–6.

Hohl, M., and Schopfer, P. (1991). Water relations of growing maize coleoptiles : comparison between mannitol and polyethylene glycol 6000 as external osmotica for adjusting turgor pressure. Plant Physiol. *95*, 716–722.

Hong, J.H., Chu, H., Zhang, C., Ghosh, D., Gong, X., and Xu, J. (2015). A quantitative analysis of stem cell homeostasis in the Arabidopsis columella root cap. Front. Plant Sci. *6*, 206.

Hsu, Y.C., and Fuchs, E. (2012). A family business: stem cell progeny join the niche to regulate homeostasis. Nat. Rev. Mol. Cell Biol. *13*, 103–114.

Hugly, S., and Somerville, C. (1992). A role for membrane lipid polyunsaturation in chloroplast biogenesis at low temperature. Plant Physiol. *99*, 197–202.

Koukalová, B., Kovarík, A., Fajkus, J., and Siroký, J. (1997). Chromatin fragmentation associated with apoptotic changes in tobacco cells exposed to cold stress. FEBS Lett. *414*, 289–292.

Kratsch, H.A., and Wise, R.R. (2000). The ultrastructure of chilling stress. Plant Cell Environ. *23*, 337–350.

Ludwig-Müller, J. (2015). Bacteria and fungi controlling plant growth by manipulating auxin: balance between development and defense. J. Plant Physiol. *172*, 4–12.

Lyons, J.M. (1973). Chilling Injury in Plants. Annu. Rev. Plant Physiol. *24*, 445–466.

Ma, K.-W., and Ma, W. (2016). Phytohormone pathways as targets of pathogens to facilitate infection. Plant Mol. Biol. *91*, 713–725.

MacMillan, H.A., Baatrup, E., and Overgaard, J. (2015). Concurrent effects of cold and hyperkalaemia cause insect chilling injury. Proc. Biol. Sci. *282*, 20151483.

Mah, L.J., El-Osta, A., and Karagiannis, T.C. (2010). gammaH2AX: a sensitive molecular marker of DNA damage and repair. Leukemia *24*, 679–686.

Maréchal, A., and Zou, L. (2013). DNA damage sensing by the ATM and ATR kinases. Cold Spring Harb. Perspect. Biol. *5*, a012716.

Mironova, V.V., Omelyanchuk, N.A., Novoselova, E.S., Doroshkov, A.V., Kazantsev, F.V., Kochetov, A.V., Kolchanov, N.A., Mjolsness, E., and Likhoshvai, V.A. (2012). Combined in silico/in vivo analysis of mechanisms providing for root apical meristem self-organization and maintenance. Ann. Bot. (Lond.) *110*, 349–360.

Morel, J.B., and Dangl, J.L. (1997). The hypersensitive response and the induction of cell death in plants. Cell Death Differ. *4*, 671–683.

Mori, M., Watanabe, M., Shiogama, H., Inoue, J., and Kimoto, M. (2014). Robust Arctic sea-ice influence on the frequent Eurasian cold winters in past decades. Nat. Geosci. *7*, 869–873.

Morishita, S., Nishi, Y., Sato, E.F., Yamaoka, K., Manabe, M., and Inoue, M. (1997). Cold-stress induces thymocyte apoptosis in the rat. Pathophysiology *4*, 213–219.

Murakami, K., Kondo, T., Yang, G., Chen, S.F., Morita-Fujimura, Y., and Chan, P.H. (1999). Cold injury in mice: a model to study mechanisms of brain edema and neuronal apoptosis. Prog. Neurobiol. *57*, 289–299.

Naseem, M., Kaltdorf, M., and Dandekar, T. (2015). The nexus between growth and defence signalling: auxin and cytokinin modulate plant immune response pathways. J. Exp. Bot. *66*, 4885–4896.

Ning, S.B., Song, Y.C., and Damme Pv, Pv. (2002). Characterization of the early stages of programmed cell death in maize root cells by using comet assay and the combination of cell electrophoresis with annexin binding. Electrophoresis *23*, 2096–2102.

Nishimura, T., Hayashi, K., Suzuki, H., Gyohda, A., Takaoka, C., Sakaguchi, Y., Matsumoto, S., Kasahara, H., Sakai, T., Kato, J., et al. (2014). Yucasin is a potent inhibitor of YUCCA, a key enzyme in auxin biosynthesis. Plant J. *77*, 352–366.

Overland, J.E., Dethloff, K., Francis, J.A., Hall, R.J., Hanna, E., Kim, S.-J., Screen, J.A., Shepherd, T.G., and Vihma, T. (2016). Nonlinear response of mid-latitude weather to the changing Arctic. Nat. Clim. Chang. *6*, 992–999.

Paciorek, T., Sauer, M., Balla, J., Wiśniewska, J., and Friml, J. (2006). Immunocytochemical technique for protein localization in sections of plant tissues. Nat. Protoc. *1*, 104–107.

Sabatini, S., Beis, D., Wolkenfelt, H., Murfett, J., Guilfoyle, T., Malamy, J., Benfey, P., Leyser, O., Bechtold, N., Weisbeek, P., and Scheres, B. (1999). An auxin-dependent distal organizer of pattern and polarity in the Arabidopsis root. Cell *99*, 463–472.

Sablowski, R. (2004). Plant and animal stem cells: conceptually similar, molecularly distinct? Trends Cell Biol. *14*, 605–611.

Scheres, B. (2007). Stem-cell niches: nursery rhymes across kingdoms. Nat. Rev. Mol. Cell Biol. *8*, 345–354.

Scheres, B., Benfey, P., and Dolan, L. (2002). Root development. Arabidopsis Book *1*, e0101.

Schwab, R., Ossowski, S., Riester, M., Warthmann, N., and Weigel, D. (2006). Highly specific gene silencing by artificial microRNAs in Arabidopsis. Plant Cell *18*, 1121–1133.

Seki, M., Narusaka, M., Ishida, J., Nanjo, T., Fujita, M., Oono, Y., Kamiya, A., Nakajima, M., Enju, A., Sakurai, T., et al. (2002). Monitoring the expression profiles of 7000 Arabidopsis genes under drought, cold and high-salinity stresses using a full-length cDNA microarray. Plant J. *31*, 279–292.

Shepherd, T.G. (2016). Effects of a warming Arctic. Science *353*, 989–990.

Shibasaki, K., Uemura, M., Tsurumi, S., and Rahman, A. (2009). Auxin response in Arabidopsis under cold stress: underlying molecular mechanisms. Plant Cell *21*, 3823–3838.

Siminovitch, D., and Cloutier, Y. (1983). Drought and freezing tolerance and adaptation in plants: some evidence of near equivalences. Cryobiology *20*, 487–503.

Slovak, R., Göschl, C., Su, X., Shimotani, K., Shiina, T., and Busch, W. (2014). A Scalable Open-Source Pipeline for Large-Scale Root Phenotyping of Arabidopsis. Plant Cell *26*, 2390–2403.

Song, J., and Bent, A.F. (2014). Microbial pathogens trigger host DNA double-strand breaks whose abundance is reduced by plant defense responses. PLoS Pathog. *10*, e1004030.

Steponkus, P.L. (1979). A unified concept of stress in plants? Basic Life Sci. *14*, 235–255.

Sung, S., and Amasino, R.M. (2005). Remembering winter: toward a molecular understanding of vernalization. Annu. Rev. Plant Biol. *56*, 491–508.

Tameshige, T., Fujita, H., Watanabe, K., Toyokura, K., Kondo, M., Tatematsu, K., Matsumoto, N., Tsugeki, R., Kawaguchi, M., Nishimura, M., and Okada, K. (2013). Pattern dynamics in adaxial-abaxial specific gene expression are modulated by a plastid retrograde signal during Arabidopsis thaliana leaf development. PLoS Genet. *9*, e1003655.

Thomashow, M.F. (1999). Plant cold acclimation: freezing tolerance genes and regulatory mechanisms. Annu. Rev. Plant Physiol. Plant Mol. Biol. *50*, 571–599.

Ühlken, C., Horvath, B., Stadler, R., Sauer, N., and Weingartner, M. (2014). MAIN-LIKE1 is a crucial factor for correct cell division and differentiation in Arabidopsis thaliana. Plant J. *78*, 107–120.

Vieten, A., Vanneste, S., Wisniewska, J., Benková, E., Benjamins, R., Beeckman, T., Luschnig, C., and Friml, J. (2005). Functional redundancy of PIN

proteins is accompanied by auxin-dependent cross-regulation of PIN expression. Development *132*, 4521–4531.

Wang, J., Sun, Q., Morita, Y., Jiang, H., Gross, A., Lechel, A., Hildner, K., Guachalla, L.M., Gompf, A., Hartmann, D., et al. (2012). A differentiation checkpoint limits hematopoietic stem cell self-renewal in response to DNA damage. Cell *148*, 1001–1014.

Xin, Z., and Browse, J. (1998). Eskimo1 mutants of Arabidopsis are constitutively freezing-tolerant. Proc. Natl. Acad. Sci. USA *95*, 7799–7804.

Xu, J., and Scheres, B. (2005). Dissection of Arabidopsis ADP-RIBOSYLATION FACTOR 1 function in epidermal cell polarity. Plant Cell *17*, 525–536.

Xu, J., Hofhuis, H., Heidstra, R., Sauer, M., Friml, J., and Scheres, B. (2006). A molecular framework for plant regeneration. Science *311*, 385–388.

Zhang, X., Henriques, R., Lin, S.S., Niu, Q.W., and Chua, N.H. (2006). Agrobacterium-mediated transformation of Arabidopsis thaliana using the floral dip method. Nat. Protoc. *1*, 641–646.

Zhang, Y., Zheng, L., Hong, J.H., Gong, X., Zhou, C., Pérez-Pérez, J.M., and Xu, J. (2016). Topoisomerase1α ACTS THROUGH TWO DISTINCT MECHANISMS TO REGULATe Stele and Columella stem cell maintenance. Plant Physiol. *171*, 483–493.

Please cite this article in press as: Hong et al., A Sacrifice-for-Survival Mechanism Protects Root Stem Cell Niche from Chilling Stress, Cell (2017), http://dx.doi.org/10.1016/j.cell.2017.06.002

STAR★METHODS

KEY RESOURCES TABLE

REAGENT or RESOURCE	SOURCE	IDENTIFIER
Antibodies		
Phospho-Histone H2A.X (Ser139) (20E3) Rabbit mAb	Cell Signaling Technology	#9718S; RRID: AB_2118009
Donkey anti-Rabbit IgG (H+L) Highly Cross-Adsorbed Secondary Antibody, Alexa Fluor 488	ThermoFisher	A-21206; RRID: AB_2535792
Chemicals, Peptides, and Recombinant Proteins		
Propidium Iodide (PI)	Sigma-Aldrich	P4170
Indole-3-Acetic Acid (IAA)	Duchefa	I0901.0100
Dexamethasone (DEX)	Sigma-Aldrich	D1756
Yucasin	Sigma-Aldrich	573760
Zeocin	ThermoFisher	R25001
Indole-3-Acetamide (IAM)	Sigma-Aldrich	286281
Critical Commercial Assays		
Click-iT EdU Alexa Fluor 647 Imaging Kit	ThermoFisher	C10340
TUNEL assay kit	Roche	11684795910
Experimental Models: Organisms/Strains		
Arabidopsis: *PIN1::PIN1-GFP*	Xu et al., 2006	N/A
Arabidopsis: *PIN2::PIN2-GFP*	Xu and Scheres, 2005	N/A
Arabidopsis: *PIN3::PIN3-GFP*	Dello Ioio et al., 2008	N/A
Arabidopsis: *PIN4::PIN4-GFP*	Blilou et al., 2005	N/A
Arabidopsis: *PIN7::PIN7-GFP*	Blilou et al., 2005	N/A
Arabidopsis: *PIN1::GUS*	Vieten et al., 2005	N/A
Arabidopsis: *PIN2::GUS*	Vieten et al., 2005	N/A
Arabidopsis: *PIN3::GUS*	Vieten et al., 2005	N/A
Arabidopsis: *PIN4::GUS*	Vieten et al., 2005	N/A
Arabidopsis: *PIN7::GUS*	Vieten et al., 2005	N/A
Arabidopsis: *DR5::GFP*	Friml et al., 2003	N/A
Arabidopsis: *WOX5::GFP*	Blilou et al., 2005	N/A
Arabidopsis: *WOX5::IAAH DR5::GFP*	Blilou et al., 2005	N/A
Arabidopsis: *J2341*	Haseloff enhancer trap GFP line	N/A
Arabidopsis: *yuc8 yuc9*	Hentrich et al., 2013	N/A
Arabidopsis: *atr*	Nottingham *Arabidopsis* Stock Centre (NASC)	SALK_054383
Arabidopsis: *wee1*	Nottingham *Arabidopsis* Stock Centre (NASC)	SALK_147968C
Arabidopsis: *atm-1*	De Schutter et al., 2007	N/A
Arabidopsis: *35S::LoxP-Ter-LoxP-VENUS*	Eriksson et al., 2010	N/A
Arabidopsis: *PIN3::CRE-GR 35S::LoxP-Ter-LoxP-VENUS*	This paper	N/A
Arabidopsis: *ACR4::GVG*	This paper	N/A
Arabidopsis: *ACR4::GVG UAS::ATRi*	This paper	N/A
Arabidopsis: *ACR4::GVG UAS::ATMi*	This paper	N/A
Arabidopsis: *ACR4::GVG UAS::WEE1i*	This paper	N/A
Oligonucleotides		
Primers used in this study, see Table S1	This paper	N/A
Recombinant DNA		
CG35ST_SKattB1-2	Tameshige et al., 2013	N/A
pGreenII-CRE-GR	This paper	N/A

(*Continued on next page*)

Continued

REAGENT or RESOURCE	SOURCE	IDENTIFIER
PIN3::CRE-GR	This paper	N/A
ACR4::GVG	This paper	N/A
UAS::ATRi	This paper	N/A
UAS::ATMi	This paper	N/A
UAS::WEE1i	This paper	N/A
Software and Algorithms		
ImageJ	NIH	https://imagej.nih.gov/ij/
Algorithms used in mathematical models in this study, see Data S1.	This paper	N/A

CONTACT FOR REAGENT AND RESOURCE SHARING

Further information and requests for resources and reagents should be directed to and will be fulfilled by the Lead Contact, Jian Xu (dbsxj@nus.edu.sg).

EXPERIMENTAL MODEL AND SUBJECT DETAILS

Arabidopsis

All *Arabidopsis* used are in the Col-0 background. Seedlings were germinated on half-strength Murashige and Skoog (MS) agar plates with 50μg/ml ampicillin incubated in a near vertical position at 22°C under long-day conditions (16 hr of light / 8 hr of darkness). Chilling treatment was performed by maintaining 6-day-old seedlings at 4°C for 24 hr. Freezing experiments were conducted by incubating Petri dishes with the seedlings in icy water for the indicated duration, before returning to optimal growth conditions, as previously described (Xin and Browse, 1998).

METHOD DETAILS

Plasmid Construction and Plant Transformation

The *PIN3::CRE-GR 35S::LoxP-Ter-LoxP-VENUS* vector was constructed as follows: the *CRE-GR* fragment was PCR amplified from *CG35ST_SKattB1-2* (gift from Kiyotaka Okada and Toshiaki Tameshige) (Tameshige et al., 2013), verified by sequencing, and ligated into a *pGreenII-0229* (http://www.pgreen.ac.uk) vector between restriction sites XbaI and NotI. The resultant construct was designated *pGreenII-CRE-GR*. A 4750-bp promoter region of *PIN3* was then PCR amplified, verified by sequencing, and ligated into *pGreenII-CRE-GR* between ApaI and XhoI sites. The resultant *PIN3::CRE-GR* construct was transformed into *35S::LoxP-Ter-LoxP-VENUS* (Eriksson et al., 2010) (gift from Kiyotaka Okada, Toshiaki Tameshige and Michael Lenhard) plants using the floral dip method (Clough and Bent, 1998; Zhang et al., 2006). To generate *ACR4::GVG*, an 1863-bp promoter region of *ACR4* was PCR amplified, verified by sequencing, and ligated into a plasmid containing *GVG* and *UAS::ERGFP* between ACC65I and SpeI sites. The resultant construct was then transformed into WT Col-0 plants. To generate *UAS::ATRi*, *UAS::ATMi* and *UAS::WEE1i* constructs, optimal artificial microRNAs (amiRNAs) against *ATR* (GGAAGGTCCCCATGTATAT), *ATM* (TGGATCTCCTTATTTACTG) and *WEE1* (TGGACATTTCAGTCGGGTA) were designed using Web MicroRNA Designer (http://wmd3.weigelworld.org). These amiRNAs were fused individually to the XbaI site of a UAS vector and the resultant constructs were transformed into WT Col-0 plants. The positive transformants were then crossed to *ACR4::GVG* transgenic plants to obtain *ACR4::GVG-UAS::ATRi* (*ATRi*), *ACR4::GVG-UAS::ATMi* (*ATMi*) and *ACR4::GVG-UAS::WEE1i* (*WEE1i*) plants.

Chemical Treatment

IAA (Duchefa) was dissolved in ethanol to achieve a stock concentration of 0.1 μM. DEX (Sigma) was dissolved in DMSO to yield a stock concentration of 5 mM. Yucasin and IAM (Sigma) were dissolved in DMSO to yield a stock concentration of 50 μM each. Zeocin (Life Technologies) was purchased as a stock of 100 mg/ml. For IAA or yucasin treatment, seeds were sown to MS agar plates supplemented with the indicated concentration of chemicals. For Zeocin treatment, 6-day-old seedlings were transferred to liquid MS medium containing the indicated amount of the chemical and gently agitated for the indicated duration.

PI and EdU Staining

PI staining was performed as previously described (Zhang et al., 2016); the roots of the seedlings were submerged in PI (10 μg/ml) and then imaged immediately. Visualization of live and dead cells with PI staining and selection of PI-stained seedlings with or without

chilling stress-induced CSCD death were performed on a Leica TCS SP5 X confocal microscope. EdU incorporation assay was performed as previously described (Hong et al., 2015). 6-day-old seedlings were treated for 24 hr with 5 μM EdU solution unless otherwise stated. The seedlings were fixed in 3.7% (v/v) paraformaldehyde before incubation with 50 μL Click-iT 461 reaction cocktail for 1 hr. GFP and GUS intensities were measured using ImageJ.

TUNEL Assay

In Situ Cell Death Detection Kit Fluorescein (Roche) was used to perform TUNEL assay according to manufacturer's protocol with slight modifications. 7-day-old seedlings were fixed in 3.7% paraformaldehyde and 1% Triton X-100 in phosphate buffered saline (PBS) solution for 30 min. After washing, the seedlings were incubated with TUNEL reaction mixture for 1 hr at 37°C. The seedlings were washed again and imaged with a Leica TCS SP5 X confocal microscope. PBS was used as a mounting medium for imaging.

γ-H2AX Foci Assay

Immunolocalization of γ-H2AX foci was performed on whole-mount roots of *Arabidopsis* seedlings as previously described (Paciorek et al., 2006). The seedlings were fixed in 3.7% (v/v) paraformaldehyde before they were placed onto slides. Slides were probed with primary antibodies targeted at γ-H2AX (Cell Signaling Technology; #9718S) and subsequently with Alexa 488-conjugated donkey anti-rabbit secondary antibodies, followed by 4′-6-diamidino-2-phenylindole dihydrochloride staining (DAPI). Images were captured with a Zeiss LSM 510 Meta confocal microscope.

Laser Ablation

Laser ablations were performed on a Leica TCS SP5 X confocal microscope with a multi-photon laser and the FRAP WIZARD of Leica Application Suite.

Mathematical Modeling

See Data S1 for detailed information of the model.

Primers

All primers used in this study were listed in Table S1.

QUANTIFICATION AND STATISTICAL ANALYSIS

All detailed statistical details parameters of the experiments can be found in the figure legends, including the type of statistical tests used, exact value of n and what n represents. Statistical tests were performed using Microsoft Excel. In figures, asterisks denote statistical significance test as compared to the controls indicated in the figure legends. All error bars represent standard error of the mean, unless otherwise mentioned in the figure legends. Quantification of cell death area (μm^2) was conducted as previously reported (Ühlken et al., 2014), by tracing out the area of cell death (marked by PI penetrance) in individual roots using ImageJ. Root lengths were also measured by scanning the Petri dishes with seedlings using a scanner and tracing individual roots in the scanned image using the ImageJ software (https://imagej.nih.gov/ij/), Relative root growth recovery rate was calculated based on the method described previously (Slovak et al., 2014). In brief, root growth rate was first calculated from the difference of the total root lengths between two subsequent time points, which was then divided by the total root length at the initial time point of the time interval to obtain relative root growth rates. Finally, relative root growth recovery rates were calculated from the difference of the relative root growth rates between roots treated with and without chilling stress for 24 hr.

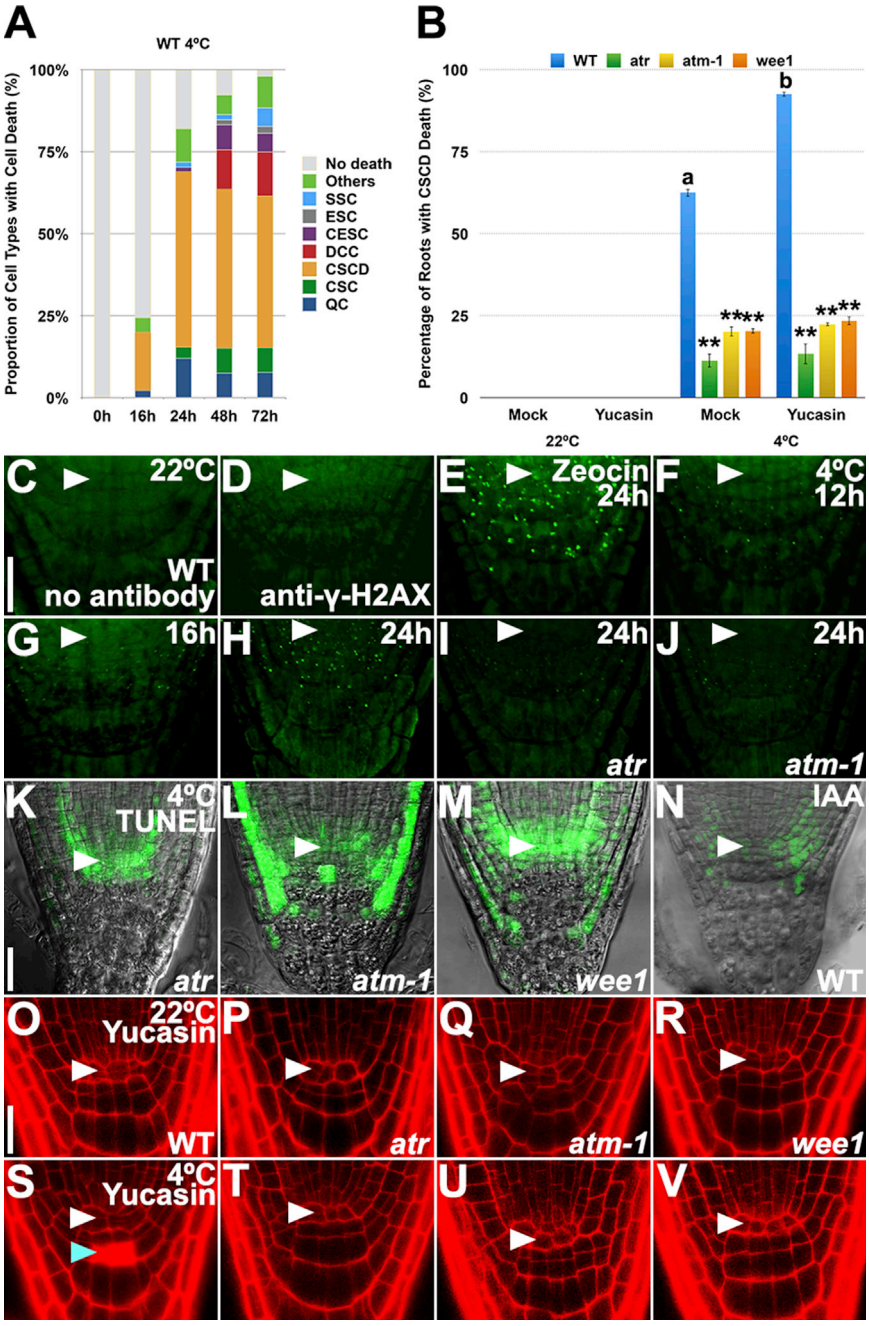

Figure S1. Chilling Stress Induces Cell Death Preferentially in CSCDs and Rapidly Induces DNA Damage and DNA Damage Response in the *Arabidopsis* Root, Related to Figure 1

(A) Chilling stress induces death of different types of cells in the *Arabidopsis* root tip. Among them, CSCDs are the most vulnerable to chilling stress. QC, quiescent center; CSC, columella stem cell; CSCD, columella stem cell daughter; DCC, differentiated columella cell; CESC, cortex and endodermis stem cell; ESC, epidermis and lateral root cap stem cell; SSC, stele stem cell.

(B) Quantification of percentage of WT, *atr*, *atm-1* and *wee1* roots with CSCD death, in the absence or presence of yucasin. WT and mutant plants were exposed to the normal (22°C; O-R) or chilling temperatures (4°C, S-V) for 24h before imaging. Note that yucasin was unable to significantly increase the percentage of mutant roots with chilling stress-induced CSCD death, as compared to the WT control. Error bars represent standard error of the mean. **$p < 0.01$ compared to the WT control by t test. Bars with different letters are significantly different at $p < 0.01$, t test. ($n = 3$ biological replicates).

(C–E) γ-H2AX foci assay of DNA damage (stained as bright green dots) in root tip cells of WT seedlings treated with mock (C, negative control; and D) or 5 μg/mL zeocin (E, positive control) for 24h at 22°C. Note that autofluorescence (in green) can be detected in root tip cells of WT seedlings in the absence of anti-γ-H2AX antibody (C). White arrowhead points to the QC. Scale bar = 20 μm.

(legend continued on next page)

(F–H) γ-H2AX foci assay of DNA damage (stained as bright green dots) in root tip cells of WT seedlings after exposure to chilling temperature (4°C) for 12h (F), 16h (G), and 24h (H). White arrowhead points to the QC. Scale bar = 20 μm.
(I and J) γ-H2AX foci assay of DNA damage (stained as bright green dots) in root tip cells of *atr* (I) and *atm-1* (J) seedlings after exposure to chilling temperature (4°C) for 24h. White arrowhead points to the QC. Scale bar = 20 μm.
(K–N) TUNEL assay of DNA fragmentation (stained in green) in root tip cells of *atr* (K), *atm-1* (L), *wee1* (M), and IAA-treated (N) seedlings after exposure to chilling temperature (4°C) for 24h. White arrowhead points to the QC. Scale bar = 20 μm.
(O–R) Root tips of yucasin (50 nM)-treated WT (O and S), *atr* (P and T), *atm-1* (Q and U), *wee1* (R and V) seedlings exposed to the normal (22°C; O-R) or chilling temperatures (4°C, S-V) for 24h. White arrowhead points to the QC and blue arrowhead points to the dead CSCDs. Scale bar = 20 μm.

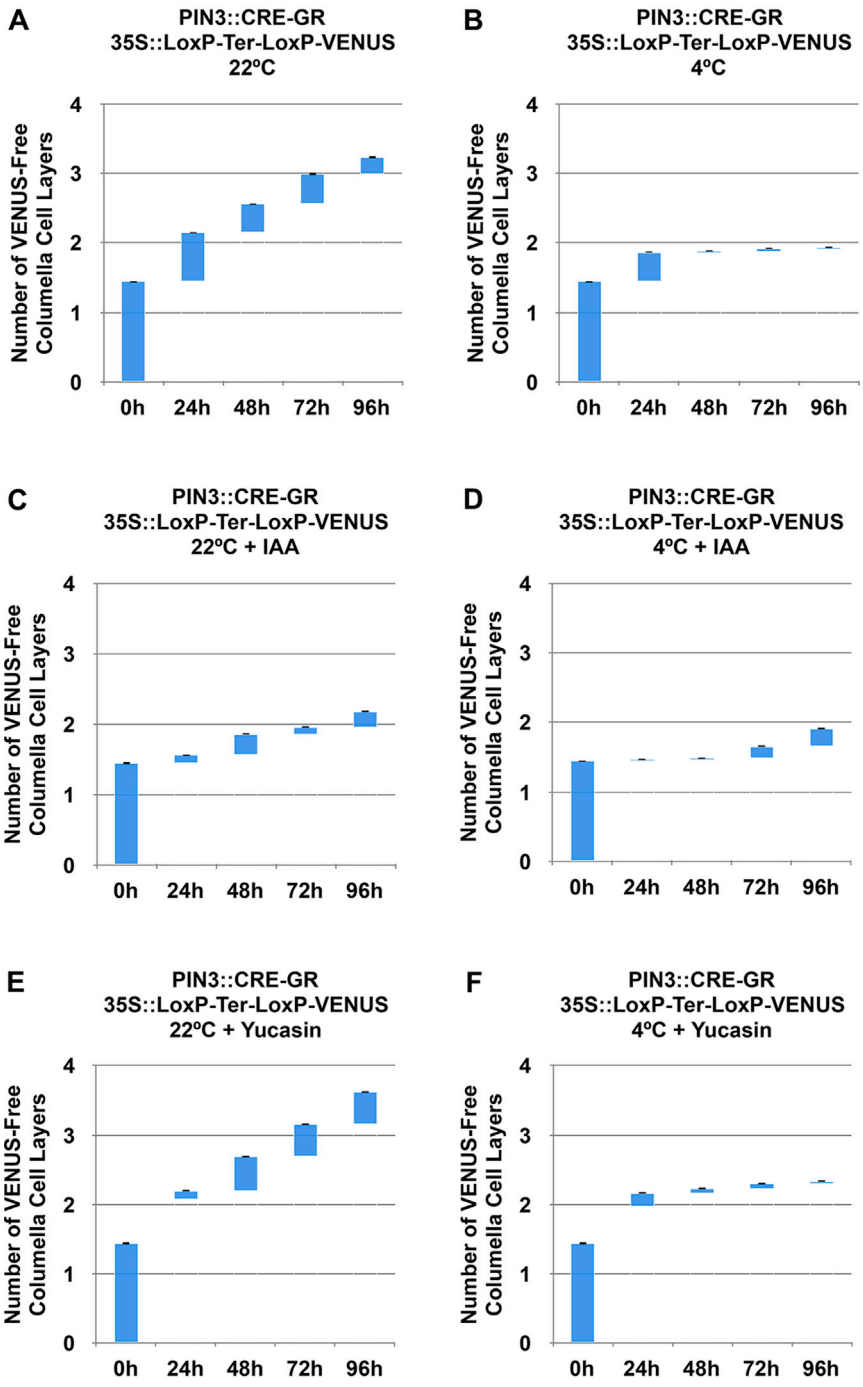

Figure S2. Auxin Levels in the Root Tip Are Decisive for CSC Division, Related to Figure 2

(A–F) Quantification of numbers of VENUS-free columella cell layers in roots of *PIN3::CRE-GR 35S::LoxP-Ter-LoxP-VENUS* seedlings treated with mock (A and B), 1 nM IAA (C and D) or 50 nM yucasin (E and F). These seedlings were transferred to DEX-free medium after the induction of VENUS expression with 5μM DEX at 22°C and allowed to grow at 22°C or 4°C for the indicated time period. Error bars represent standard error of the mean. (n = 3 biological replicates).

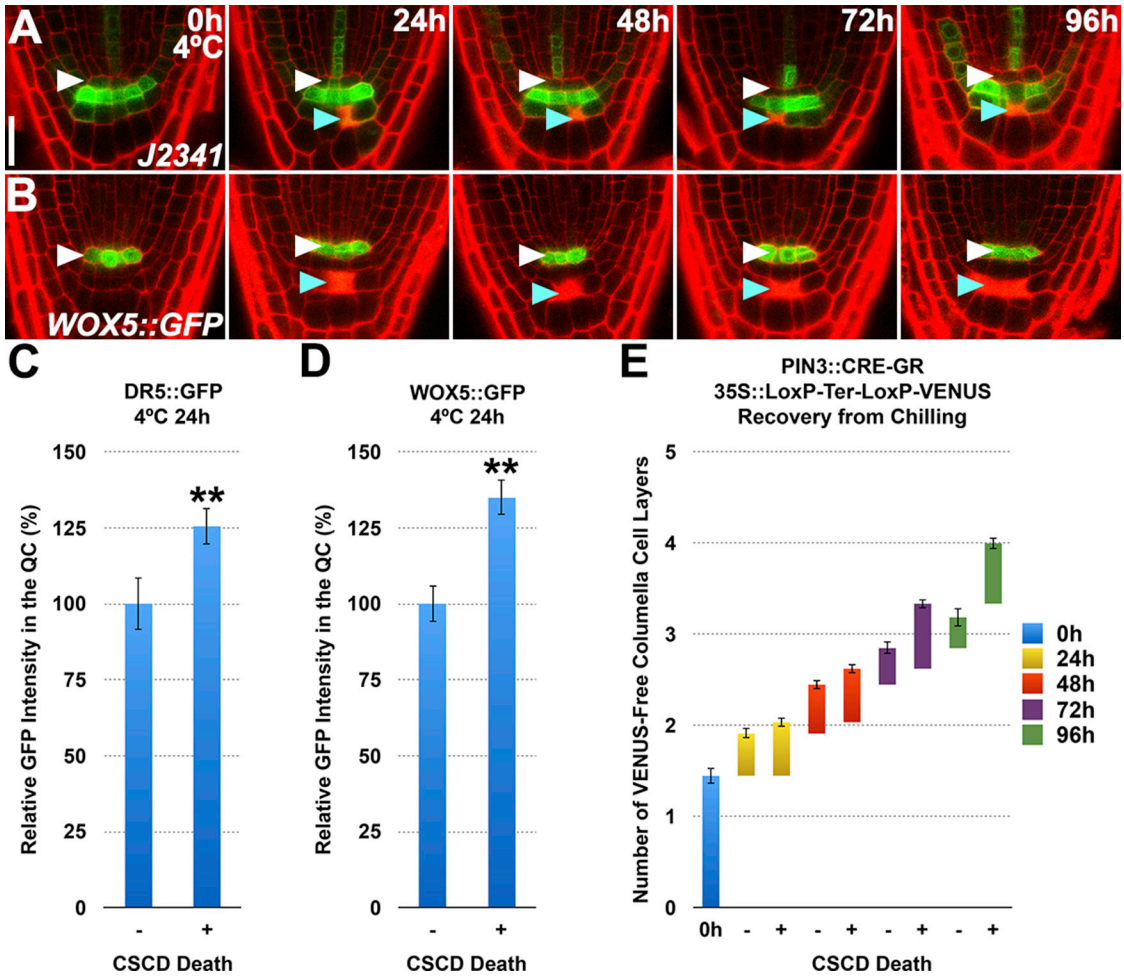

Figure S3. Chilling Stress Does Not Affect the Cell-Specific Expression Pattern of CSC and QC Markers, and Death of CSCDs Increases *DR5::GFP* and *WOX5::GFP* Expression in the QC and Renders Faster CSC Division during Recovery from Chilling Stress, Related to Figures 2 and 5

(A and B) Expression of the CSC marker *J2341* (A) and the QC marker *WOX5::GFP* (B) in roots at the indicated period of time following chilling stress (4°C). White arrowhead points to the QC and blue arrowhead points to the dead CSCDs. Scale bar = 25 μm.

(C and D) Quantification of expression of *DR5::GFP* (C) and *WOX5::GFP* (D) in the QC of *Arabidopsis* roots without (-) or with (+) chilling stress-induced CSCD death. Error bars represent standard error of the mean. **$p < 0.01$, t test. (n = 3 biological replicates).

(E) *PIN3::CRE-GR 35S::LoxP-Ter-LoxP-VENUS* seedlings were transferred to DEX-free medium after the induction of VENUS expression with 5μM DEX at 22°C and chilling-stressed at 4°C for 24h. The seedlings without (-) and without (+) chilling stress-induced CSCD death were then allowed to recover at 22°C for the indicated period of time before quantification of numbers of VENUS-free columella cell layers. Error bars represent standard error of the mean. (n = 3 biological replicates).

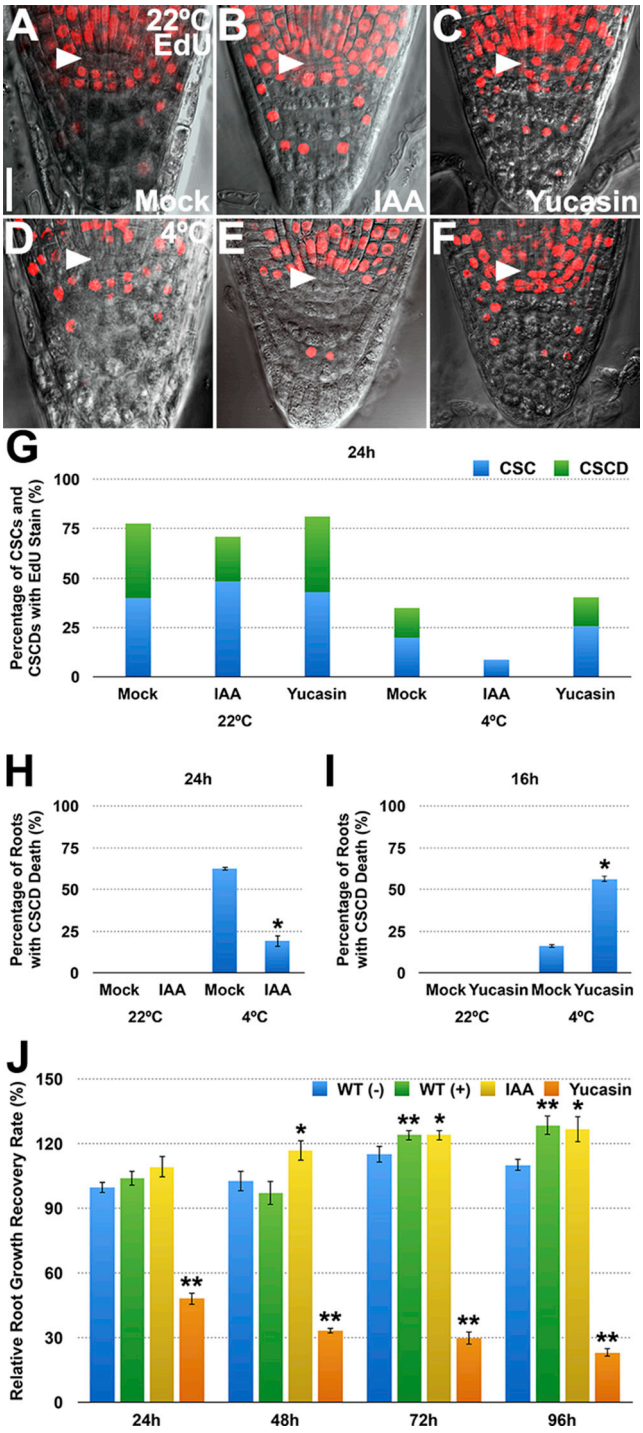

Figure S4. Auxin Levels in the Root Tip Are Decisive for the Induction of CSC Division and CSCD Death and for Root Growth Recovery after Chilling Stress, Related to Figures 2 and 6

(A–F) EdU staining pattern in root tips of WT seedlings treated with mock (A and B), 1 nM IAA (C and D) or 50 nM yucasin for 24h at 22°C (A-C) or 4°C (D-F). White arrowhead points to the QC. Scale bar = 25 μm.

(G) Quantification of percentage of CSCs and CSCDs with EdU stain. Note that 1 nM IAA reduced whereas 50 nM yucasin increased EdU stain in chilling-stressed CSCs.

(H and I) Quantification of the CSCD death phenotype in roots exposed to chilling stress at 4°C for 24h (H) and 16h (I). Error bars represent standard error of the mean. *$p < 0.05$, t test. (n = 3 biological replicates).

(legend continued on next page)

(J) Time course analysis of relative root growth recovery rate during recovery from chilling stress. mock-, IAA (1 nM)- and yucasin (50 nM)-treated WT seedlings grown at 22°C were chilling-stressed at 4°C for 24h and then allowed to recover at 22°C for the indicated period of time. Relative root growth recovery rate of WT (-, without chilling stress-induced CSCD death) seedlings at 24h after chilling stress was set to 100%. Error bars represent standard error of the mean. *$p < 0.05$, **$p < 0.01$, t test. (n = 3 biological replicates).

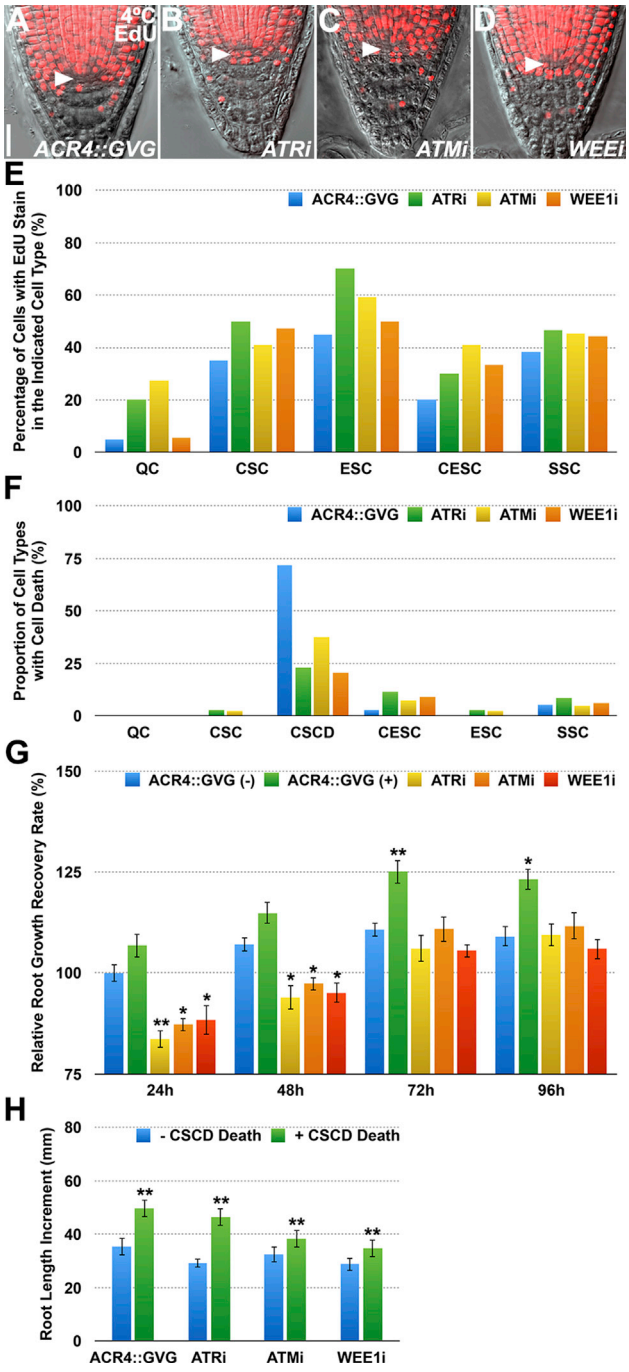

Figure S5. Death of CSCDs Is Used to Protect the Root Stem Cell Niche and Help Roots Recover Faster from Chilling Stress, Related to Figures 5 and 6

(A–D) EdU staining pattern in root tips of DEX (5 μM)-treated *ACR4::GVG* (A), *ACR4::GVG-UAS::ATRi* (*ATRi*) (B), *ACR4::GVG-UAS::ATMi* (*ATMi*) (C) and *ACR4::GVG-UAS::WEE1i* (*WEE1i*) (D) seedlings at 24h following chilling stress. White arrowhead points to the QC. Scale bar = 25 μm.

(E) Quantification of percentage of chilling-stressed QC and root stem cells with EdU staining. Note that DEX-induced knockdown of *ATR*, *ATM* and *WEE1* in *ACR4*-expressing cells largely increases EdU stain in the root stem cell niche, as compared to that of *ACR4::GVG*. (n = 3 biological replicates).

(F) DEX (5 μM)-treated *ATRi*, *ATMi* and *WEE1i* seedlings display reduced CSCD death at 24h following chilling stress, as compared to *ACR4::GVG*, but the proportion of death in root stem cells increases. (n = 3 biological replicates).

(G) Time course analysis of relative root growth recovery rate during recovery from chilling stress. *ACR4::GVG*, *ATRi*, *ATMi*, *WEE1i* seedlings grown at 22°C with 5 μM DEX were chilling-stressed at 4°C for 24h and then allowed to recover at 22°C for the indicated period of time. Relative root growth recovery rate of

(legend continued on next page)

ACR::GVG (-, without chilling stress-induced CSCD death) seedlings at 24h after chilling stress was set to 100%. Error bars represent standard error of the mean. *p < 0.05, **p < 0.01, t test. (n = 3 biological replicates).

(H) Quantification of root length increment during recovery period. *ACR4::GVG*, *ACR4::GVG-UAS::ATRi* (*ATRi*), *ACR4::GVG-UAS::ATMi* (*ATMi*) and *ACR4::GVG-UAS::WEE1i* (*WEE1i*) seedlings grown at 22°C were chilling-stressed at 4°C for 24h, followed by freezing treatment at 0°C for 7d, and then allowed to recover at 22°C for 7d. DEX (5 μM) was applied at all stages of seedling growth to induce knockdown of *ATR*, *ATM* and *WEE1* in *ACR4*-expressing cells. Error bars represent standard error of the mean. **p < 0.01, t test. (n = 3 biological replicates).

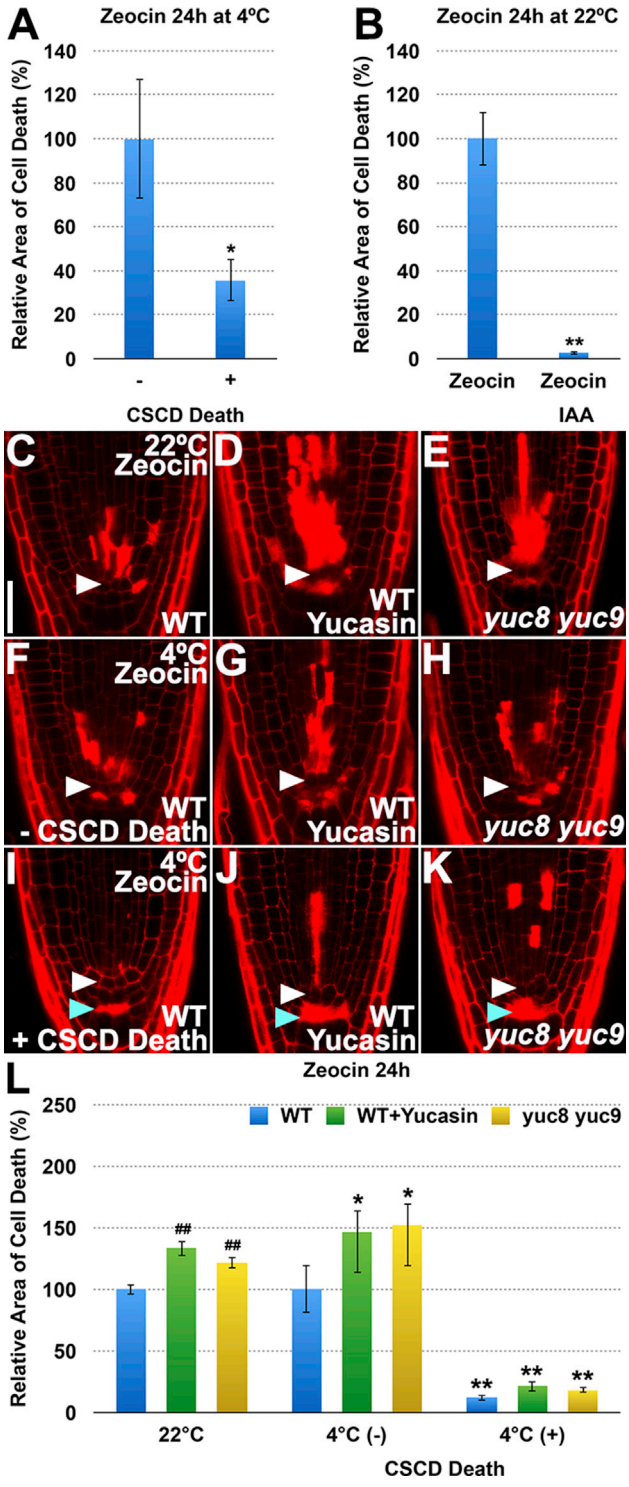

Figure S6. Death of CSCDs and Auxin Render Better Tolerance to Zeocin Whereas Genetic and Pharmacological Disruption of YUC-Dependent Auxin Biosynthesis Sensitizes Root Stem Cells to Zeocin, Related to Figure 5

(A) Quantification of zeocin-induced death of cells in the root stem cell niche of seedlings without (-) or with (+) chilling stress-induced CSCD death. Following 24h of chilling stress at 4°C, these seedlings were treated with 30 μg/ml zeocin at 4°C for 24h before quantification. Error bars represent standard error of the mean. *$p < 0.05$, t test. (n = 3 biological replicates).

(B) Quantification of zeocin-induced death of cells in the root stem cell niche of seedlings treated with 5 μg/mL zeocin or 5 μg/mL zeocin and 50 nM IAA for 24h at 22°C. Error bars represent standard error of the mean. **$p < 0.01$, t test. (n = 3 biological replicates).

(legend continued on next page)

(C–E) Root tips of WT (C and D) and *yuc8 yuc9* (E) seedlings treated with 5 μg/mL zeocin (C and E) or 5 μg/mL zeocin and 200 nM yucasin (D) for 24h at 22°C. White arrowhead points to the QC. Scale bar = 20 μm.

(F–K) Root tips of WT (F, G, I and J) and *yuc8 yuc9* (H and K) seedlings treated with 30 μg/mL zeocin (F, H, I and K) or 30 μg/mL zeocin and 200 nM yucasin (G and J) for 24h at 4°C. (F-H) Root tips without chilling stress-induced CSCD death. (I-K) Root tips with chilling stress-induced CSCD death. White arrowhead points to the QC and blue arrowhead points to the dead CSCDs, respectively.

(L) Quantification of zeocin-induced death of cells in the root stem cell niche of seedlings without (-) or with (+) chilling stress-induced CSCD death. Error bars represent standard error of the mean. ## $p < 0.01$, compared to the WT control at 22°C, t test. *$p < 0.05$, **$p < 0.01$, compared to the WT control at 4°C, t test. (n = 3 biological replicates).

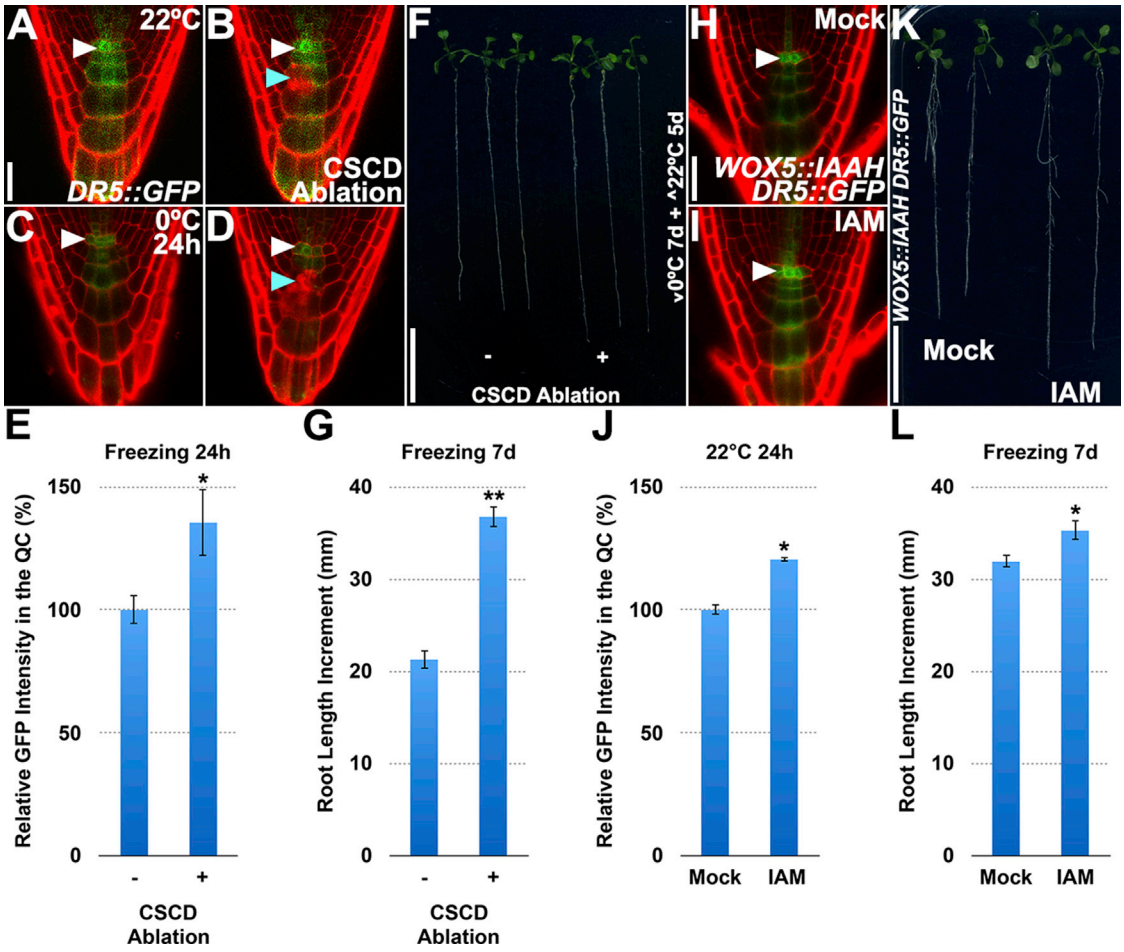

Figure S7. CSCD Ablation and Induction of QC-Specific Auxin Biosynthesis Renders Better Recovery of Root Growth after Freezing Stress, Related to Figure 6

(A and B) Expression of *DR5::GFP* immediately before and after CSCD ablation at 22°C. White arrowhead points to the QC. Scale bar = 20 μm.

(C and D) Expression of *DR5::GFP* after freezing treatment at 0°C for 24h. White arrowhead points to the QC and blue arrowhead points to the ablated CSCDs.

(E) Quantification of expression of *DR5::GFP* in the QC of *Arabidopsis* roots without (-) or with (+) CSCD ablation. Error bars represent standard error of the mean. *$p < 0.05$, t test. (n = 3 biological replicates).

(F) *DR5::GFP* seedlings without (-) or with (+) CSCD ablation. Following CSCD ablation at 22°C, these seedlings were freezing-stressed at 0°C for 7 days and then allowed to recover at 22°C for another 5 days before imaging. Scale bar = 20 mm.

(G) Quantification of root length increment 5 days after recovery from freezing treatment. Error bars represent standard error of the mean. **$p < 0.01$, t test. (n = 3 biological replicates).

(H and I) Expression of *DR5::GFP* in *WOX5::IAAH DR5::GFP* roots treated with mock or 1 nM IAM for 24h at 22°C. White arrowhead points to the QC. Scale bar = 20 μm.

(J) Quantification of expression of *DR5::GFP* in the QC of *WOX5::IAAH DR5::GFP* roots treated with mock or 1 nM IAM for 24h at 22°C. Error bars represent standard error of the mean. *$p < 0.05$, t test. (n = 3 biological replicates).

(K) *WOX5::IAAH DR5::GFP* seedlings treated with mock or 1 nM IAM. Following 24h of mock or IAM treatment at 22°C, these seedlings were freezing-stressed at 0°C for 7 days and then allowed to recover at 22°C for another 5 days before imaging. Scale bar = 20 mm.

(L) Quantification of root length increment 5 days after recovery from freezing treatment. Error bars represent standard error of the mean. *$p < 0.05$, t test. (n = 3 biological replicates).